Indoor Air

SPECIAL ISSUE Emerging Digital Technologies and Trends for Enhancing Indoor Air Quality

WILEY

RESEARCH ARTICLE OPEN ACCESS

Performance Evaluation of an AI-Based Model Predictive Control Algorithm for Outdoor Air-Based Ventilation Systems in Elementary School Facilities

Jae Yoon Byun[1] | Tae Won Kim[2] | Ji Young Yun[2] | Geun Young Yun[3] | Jin Woo Moon[2]

[1]College of Design, North Carolina State University, Raleigh, North Carolina, USA | [2]School of Architecture and Building Science, Chung-Ang University, Seoul, Republic of Korea | [3]Department of Architectural Engineering, Kyung Hee University, Yongin-si, Gyeonggi-do, Republic of Korea

Correspondence: Jin Woo Moon (gilerbert73@cau.ac.kr)

Received: 19 November 2025 | **Revised:** 7 April 2026 | **Accepted:** 8 April 2026

Guest Editor: Abdollah Baghaei Daemei

ABSTRACT

Improvements in the indoor environment at schools are required due to the long periods of time spent in school facilities by children, who are particularly vulnerable to poor indoor air quality (IAQ). This study thus developed an AI-based model predictive control algorithm (MPCA) for an outdoor air-based energy recovery ventilation (ERV) system and evaluated its performance. The MPCA was based on artificial neural networks that predicted the particulate matter (PM) concentration, carbon dioxide (CO_2) levels, and temperature to achieve real-time IAQ control. This algorithm was employed in an elementary school facility, and its performance was empirically compared with a rule-based algorithm and occupant discretionary control (ODC). All three methods were able to improve the IAQ, with the proposed MPCA outperforming the rule-based algorithm by maintaining a 21% lower $PM_{2.5}$ concentration and 7% lower CO_2 concentration. In addition, ODC required 2.4–2.5 times higher energy consumption than the other control methods, whereas the MPCA achieved a 5.7% reduction in energy consumption compared with the rule-based algorithm. Therefore, the MPCA developed in this study is capable of predictive IAQ control for ERV systems and requires less energy than conventional methods, demonstrating its potential to effectively improve the IAQ of school facilities.

1 | Introduction

It has been estimated that individuals in modern society spend approximately 80%–90% of their day indoors [1, 2], which means that it is important to maintain safe and comfortable indoor environments [3, 4]. To achieve this, managing indoor air quality (IAQ) is essential [5], especially for adolescents and children, who exhibit greater sensitivity to contaminants and thermal stress in indoor air [6]. In particular, infants and young children react more sensitively to contaminants because they breathe in more air per unit body weight and have less robust immune systems and a smaller body-mass-to-surface-area ratio than adults, while they are also more vulnerable to heat stress [6–9]. Schools, where children spend extended periods engaging in educational activities, often have five times the occupancy density of office spaces and eight times that of residential spaces, increasing the likelihood of indoor air contamination [10–12]. Thus, improving the environmental quality of school facilities via IAQ management is required to protect the health of students.

To improve the IAQ of school facilities, governments in a number of countries have proposed various legal guidelines [13–20]. For example, the Republic of Korea has established environmental management standards and guidelines across several governmental departments. The Ministry of Environment in Korea enacted the Indoor Air Quality Control Act in 2004, with its 20th amendment in 2022, which defines 17 IAQ contaminants—including carbon dioxide (CO_2), particulate matter (PM), and formaldehyde—and sets advisory maximum concentration standards for each [21]. Additionally, the Ministry of Education mandates the installation of mechanical ventilation systems in newly constructed schools as part of its PM reduction strategy, while promoting the use of mechanical ventilation systems and the installation of air purifiers in existing schools [22].

Elementary schools in Korea, which educate children aged 7–13, are classified as facilities vulnerable to IAQ contamination due to their high occupancy density, the active movement of students, and the aging of buildings, all of which contribute to higher PM levels [23]. However, an analysis of the governmental budget allocated for improving the environment of school facilities conducted by the National Assembly revealed that 99.2% of funds were allocated to the installation of individual air purifiers rather than mechanical ventilation systems. [24] This is due to a common misconception shared by educators that air purifiers are much easier to install and are sufficiently effective, while they also have less trust in mechanical ventilation [24]. The automated control of individual air purifiers is limited to setting operating schedules, meaning that teachers must repeatedly turn the devices on and off during class hours, disrupting lessons. Although numerous strategies, including the use of newer technologies such as multidomain smart control and variable speed drives, have been proposed to solve this problem, many limitations remain, such as a lack of automated optimal control and systematic inflexibility [25]. Furthermore, conventional air purifiers are limited in their ability to preemptively manage primary IAQ contaminants such as PM and CO_2 in school facilities.

In this context, to ensure efficient integrated control, a ventilation system control algorithm capable of optimal IAQ control is required. This form of optimal control requires accurate and stable predictions across various scenarios based on prediction models that can account for real-time variation in contaminant levels [26]. IAQ prediction, which requires nonlinear data forecasting, can be effectively handled using prediction model algorithms such as artificial neural networks (ANNs), fuzzy theory, and regression models. Previous studies by Kim and Hong [27] and Lagesse et al. [28] have demonstrated that ANN models are particularly well-suited to parallel distributed processing, offering faster computational processing speeds and adaptive learning capabilities. These benefits give them a significant advantage in terms of predictive accuracy for IAQ contaminant concentrations.

Previous studies on IAQ control algorithms for school facilities have targeted ventilation and air purification systems, such as windows or HVAC equipment, to manage IAQ contaminants, and most of these studies have focused on controlling single contaminants, such as CO_2 or PM. For example, Choi and Lee [29] developed a window operating algorithm for the management of CO_2 levels in secondary school facilities using computer simulation modeling tools such as Energy Plus. Similarly, Park et al. [30] proposed an integrated control algorithm for ventilation and air purification, conducting IAQ contaminant prediction and analysis using computer simulations. Some studies have also examined control algorithms that account for multiple contaminants. Stazi et al. [31] developed an automated window control system that optimized both IAQ and thermal comfort; however, their study primarily focused on thermal comfort and CO_2 rather than multiple IAQ contaminants, with no consideration of PM generation due to occupant activity or outdoor conditions. Cho et al. [32] also devised an intelligent HVAC control strategy for various IAQ factors within school facilities. Their study predicted various indoor environmental factors and validated the control performance using computer simulations; however, practical application was not tested, with no acquisition and verification of real-world data. This is an issue because, in simulation-based studies, discrepancies can arise between simulation results and actual field data due to various technical limitations, meaning that simulations may not fully reflect real-world phenomena [33–35].

Many studies on control algorithms have been based on computer simulations; however, recent research has introduced the use of living labs or real-world environments. Kim et al. [36] experimented with an indoor environmental monitoring system using an operational living lab, collecting actual PM and CO_2 data through Internet of Things (IoT) technology to analyze environmental behavior. Similarly, Plazas and de Tejada [37] used real environmental data to pursue occupant-based IAQ improvements and proposed a natural ventilation system. Though both studies highlighted the need for control strategies based on real data, they did not test advanced IAQ control strategies, such as the use of control algorithms or mechanical ventilation. Shang et al. [38] also introduced an intelligent air purifier control strategy with deep reinforcement learning, testing its energy efficiency and control performance in real situations, though it was only limited to air purifier control without considering natural/mechanical ventilation. El-Leathey et al. [39] developed a real-time monitoring and natural ventilation system using IoT for occupants in a real environment and validated its performance, but the enhanced control strategy was relatively limited. These previous studies were set in either residential or office spaces, thus focusing primarily on adult occupancy, and there have been few studies that address educational facilities specifically. Although Kim and Lee [40] compared indoor $PM_{2.5}$ prediction performance during occupancy based on ANN models, and Na et al. [41] optimized IAQ in old school classrooms with air purifiers and HRV, these studies and others like them have lacked real-life applications and/or empirical experiments to confirm the utility of their systems.

In line with the sustainability directives, optimal control methods should also be energy efficient. Research conducted by Jia et al. [42], Sadrizadeh et al. [43], and Al Mindeel et al. [44] has suggested that multiobjective optimization between energy and IAQ is required, especially for educational buildings such as schools. However, very few studies have considered both energy use and IAQ together. Cho et al. [32] considered energy efficiency but did not test their system in a practical application, whereas Yu et al. [45] employed an optimization strategy for IAQ and energy consumption in a real-life setting, but this was limited to a university campus classroom, which differs in its characteristics compared with educational facilities for younger occupants.

Due to these limitations of past research, the objective of this paper was to develop an AI-based model predictive control strategy for ventilation systems that can be used to effectively manage the indoor environment in school classrooms. Its performance was evaluated by employing it in an elementary school while the classroom is actually in use. For this purpose, the study developed prediction models for $PM_{2.5}$ and CO_2 concentrations and indoor temperature based on ANNs and incorporated these models into an AI-based model predictive control algorithm (MPCA) for the school ventilation system. This algorithm was then installed in a living lab setting within an operational elementary school classroom to assess the real-time IAQ improvement and energy usage. Although the HVAC system was not directly controlled in this study, a temperature prediction model was developed as a preparatory step toward future integration of model predicted control with HVAC systems. The model also served as a supplementary predictor, enabling assessment of thermal conditions alongside IAQ.

2 | Methodology

2.1 | Development of IAQ Prediction Models

2.1.1 | Control Target Selection

Of the IAQ factors designated by the School Health Act Enforcement Rules in Korea for general classrooms and cafeterias, PM and CO_2 were selected as the primary control targets due to the relative ease of their control and their significant impact on the health of occupants. PM can be categorized as PM_{10} or $PM_{2.5}$ based on the particle size; this study focused primarily on $PM_{2.5}$ as the primary target for control. [46, 47] At concentrations above 2000 ppm, CO_2 can cause immediate negative effects—such as headaches, dizziness, reduced concentration, and difficulties in breathing—which can directly impact academic performance [48]. In addition, in comparison with other contaminants such as volatile organic compounds, $PM_{2.5}$ and CO_2 can be more easily controlled by ventilation systems installed in general elementary school facilities and in living lab environments.

In the proposed control system, $PM_{2.5}$ was established as the main priority, with CO_2 as a secondary priority, based on the characteristics of the contaminants, their impact on the occupants, and control difficulty. Although CO_2 has a direct, short-term impact on occupant health, it is less hazardous than $PM_{2.5}$, which contains both toxic and allergenic organic and inorganic substances, some of which are potentially carcinogenic, and is thus considered the most dangerous contaminant in terms of long-term exposure [49–52]. In addition, $PM_{2.5}$ cannot easily be reduced through natural ventilation alone; in fact, ventilation can occasionally increase $PM_{2.5}$ levels due to the airflow resuspending particles that had already settled within the classroom, while also allowing the inflow of outdoor $PM_{2.5}$ [53]. Consequently, reducing $PM_{2.5}$ requires mechanical ventilation systems and air purification functions, with a longer time needed for effective reduction compared with CO_2 [54]. In contrast, gaseous CO_2 can be quickly reduced through simple natural ventilation by opening the windows or door.

This study focused on developing an algorithm to control energy recovery ventilation (ERV) systems in elementary school classrooms aimed at reducing IAQ contaminants. However, the HVAC system in the living-lab environment was an independent system that was not controlled by the control algorithm. Therefore, for the present study, the control of the HVAC system and thus the indoor temperature was mainly determined by the occupants, meaning that the indoor temperature was not considered a primary control target for the AI-based control algorithm. Nevertheless, the ERV system utilized in this research can also control the indoor temperature by adjusting the ERV mode, so an indoor temperature prediction model was incorporated into the proposed AI-based control algorithm in order to assess the indoor temperature as a supplementary control target for future adaptation.

2.1.2 | Development of the ANN-Based Prediction Models

This study developed prediction models for the indoor $PM_{2.5}$ and CO_2 concentrations and temperature for integration into the AI-based MPCA. Because ANNs have demonstrated greater suitability for IAQ prediction than other models [27, 28], this type of model was selected for this prediction task. ANNs can be divided into feedforward neural networks and recurrent neural networks, with their performance varying based on the application situation and prediction target [55]. Referencing prior research [26, 56, 57], this study employed a multilayer perceptron (MLP), a feedforward neural network frequently used for IAQ and PM prediction, as the basis for the prediction models.

The input variables used for the development of the prediction models were selected from key factors influencing contaminant concentrations and temperature, prioritizing those that are easily obtainable from sensor measurements. Previous research has conducted correlation analysis for various input variables, and the present study utilized the same input variables for its prediction models [57, 58]. In particular, 11 input variables were used for $PM_{2.5}$ prediction: indoor and outdoor temperature (Temp) and relative humidity (RH), indoor and outdoor $PM_{2.5}$ concentration, indoor and outdoor PM_{10} concentration, indoor and outdoor CO_2 concentration, and system airflow rate (0 = off/1 = low/2 = middle/3 = high). For CO_2 prediction, eight input variables were used: indoor and outdoor $PM_{2.5}$ concentration, indoor and outdoor PM_{10} concentration, indoor and outdoor CO_2 concentration, system airflow rate, and system mode (0 = off/OA = outdoor air intake/IA = indoor air recirculation). Temperature prediction incorporated 12 input variables: indoor and outdoor temperature and RH, indoor and outdoor CO_2 concentration, indoor and outdoor $PM_{2.5}$ concentration, indoor and outdoor PM_{10} concentration, system airflow rate, and system mode. The system mode was excluded as an input variable for the $PM_{2.5}$ prediction model because the high-efficiency particulate air (HEPA) filters in ventilation and air purification systems prevent significant differences in $PM_{2.5}$ levels depending on whether outdoor air is introduced or indoor air is recirculated. Similarly, indoor and outdoor temperature and RH were excluded from the CO_2 prediction model because they do not significantly impact CO_2 levels. The output variables for the respective models were the indoor $PM_{2.5}$ concentration, indoor CO_2 concentration, and temperature, each predicted 5 min ahead.

A dataset was constructed based on classroom data collected from the living lab using a rule-based algorithm that did not employ preemptive $PM_{2.5}$ or CO_2 control in the spring and fall semesters. The rule-based algorithm used in this process was the same algorithm employed for the comparison with the MPCA, while the living-lab classroom was also the same classroom used for the empirical experiment, with the same environment, equipment, and occupant density/schedule. Data from days with anomalies, such as those with unexpected or irrelevant events that compromised the occupational conditions, those with unrepeated data spikes, those when the control system was not in operation, and those without occupants were excluded from the dataset. Only data collected within the occupancy hours of 8:00 a.m. to 4:30 p.m. were included due to the significant influence of occupancy on the indoor temperature, humidity, and CO_2 levels and because occupant activity directly affects the PM concentration. To preserve the accuracy of the prediction models, a total of 15 days (7095 data points) selected from the 1st and 2nd semesters of the Korean academic schedule (1st semester: March to July; 2nd semester: September to December) were included in the dataset. The data points were selected from time periods where the average indoor $PM_{2.5}$ concentration during occupancy exceeded 5 $\mu g/m^3$, the CO_2 concentration was above 600 ppm, and at least two morning classes had been conducted. The dataset was normalized using MinMaxScaler, which transformed the data to a range of 0–1 based on the minimum and maximum values. This dataset was then divided into training (60%), validation (20%), and test data (20%). Details of the data are presented in Table 1.

The ANN-based temperature prediction model was included to evaluate its potential role in integrated ERV–HVAC control. Although not directly used for control in the present study, it provides a foundation for future adaptation and demonstrates the feasibility of incorporating thermal comfort into predictive IAQ management.

Bayesian optimization, a method based on Bayesian probability, was used to identify the optimal hyperparameter combinations for the prediction models. Compared with grid search and random search, Bayesian optimization offers a shorter search time and a broader search scope. This method observes the performance outcomes of randomly sampled hyperparameters and uses these observations to estimate an optimal function. This function then suggests the next hyperparameter to observe, refining the optimal function prediction. This iterative process continues until the estimated optimal function identifies the hyperparameters that achieve the target performance [59].

Because Bayesian optimization requires a predefined model structure, this study defined the structural and optimizer parameters based on hyperparameter types (Table 2). The tuner was set to explore the number of hidden layers, number of neurons, and learning rate. According to prior studies, Adam was used as the optimizer because it outperforms other stochastic gradient descent approaches in nonimage calibration-based tasks [60, 61], with ReLU employed as the activation function and the mean square error (MSE) as the loss function. The resulting ANN structure consisted of one input layer, four hidden layers, and one output layer. Each layer included 11 input nodes

TABLE 1 | Details of the dataset used for prediction model development.

		Details
Data collection period		Months selected from both the 1st semester (March–July) and 2nd semester (September–December)
Learning data selection criteria		1. Average indoor $PM_{2.5}$ concentration above 5 $\mu g/m^3$ during occupancy
		2. Average indoor CO_2 concentration above 600 ppm during occupancy
		3. Two or more sessions of indoor classes before noon
		4. Data from 8:00 am to 16:30 pm on days that meet Criteria 1, 2, and 3 excluding P.E. class and special outdoor activities
Number of data points		7095 (15 days)
Input data	$PM_{2.5}$ model	Indoor: temperature, relative humidity, CO_2, $PM_{2.5}$, and PM_{10} concentration
		Outdoor: temperature, relative humidity, CO_2, $PM_{2.5}$, and PM_{10} concentration
		System: airflow rate
	CO_2 model	Indoor: CO_2, $PM_{2.5}$, and PM_{10} concentration
		Outdoor: CO_2, $PM_{2.5}$, and PM_{10} concentration
		System: mode and airflow rate
	Temperature model	Indoor: temperature, relative humidity, CO_2, $PM_{2.5}$, and PM_{10} concentration
		Outdoor: temperature, relative humidity, CO_2, $PM_{2.5}$, and PM_{10} concentration
		System: mode and airflow rate
Output data		Indoor $PM_{2.5}$ concentration 5 min later/indoor CO_2 concentration 5 min later/indoor temperature 5 min later
Dataset classification		Training data (60%), validation data (20%), and test data (20%)
Normalization		Min–max scaling

TABLE 2 | Prediction model structure.

Hyperparameters		Details
Structural	Number of neurons for hidden layers	10–100
	Number of hidden layers	1–10
	Activation function	ReLU
	Learning rate	0.0001
Optimizer	Type of optimizer	Adam
	Batch size	32
	Number of epochs	50
	Loss function	MSE
$PM_{2.5}$ ANN structure	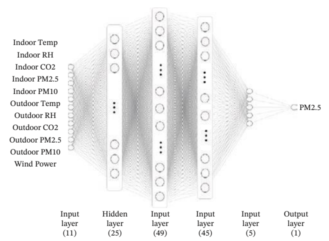	
CO_2 ANN structure	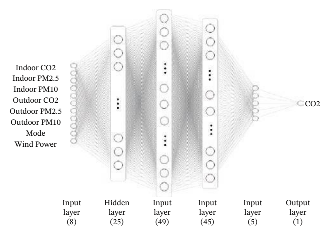	
Temperature ANN structure	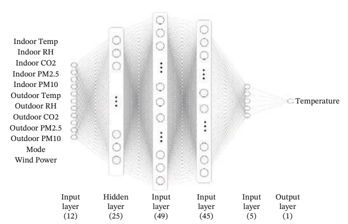	

for $PM_{2.5}$, 8 for CO_2, and 12 for temperature, with hidden nodes of 25, 49, 45, and 5, and a single output node.

The developed prediction models were integrated into the MPCA for real-time predictions, with an added self-retraining function to enhance prediction performance and facilitate adaptability to environmental changes. This continuous retraining function updated the necessary weights to correct for errors, aligning predictions more closely with the actual values and allowing the models to respond flexibly to changes. Before embedding the prediction models into the algorithm, they were retrained with recent data to validate and compare their prediction performance before and after retraining. To

TABLE 3 | Details of the data used for prediction model retraining.

	Details
Data collection period	1st academic semester of 2023
Learning data selection criteria	Same as the prediction model (see Table 1)
Number of learning data points	6327 (13 days)
Input data	Same as the prediction model (see Table 1)
Output data	Same as the prediction model (see Table 1)

retrain the prediction models, a new dataset containing more recent data than in the initial learning dataset was extracted. The selection criteria remained the same, but data from different dates were chosen. The final retraining dataset consisted of 13 days of data (6327 data points) collected between March and June 2023. Details of the retraining dataset are presented in Table 3, and the structure of the prediction models is outlined in Table 2.

The retraining process was conducted by inputting the selected retraining dataset into the $PM_{2.5}$, CO_2, and temperature prediction models. This process is aimed at comparing the performance of the models before and after retraining, ultimately selecting the model with the highest prediction performance to be included in the MPCA. After retraining, three performance metrics were calculated for each prediction model: the mean absolute error (MAE), coefficient of variation of the root mean square error (CVRMSE), and R [2]. The MAE is an intuitive measure of the absolute magnitude of error that calculates the average of the absolute error, whereas the CVRMSE measures the difference between the actual and predicted values and R^2 indicates how well the regression equation explains the original data, with values ranging from 0 to 1. Generally, lower MAE and CVRMSE values indicate greater predictive accuracy, whereas an R^2 closer to 1 represents lower error [62]. The MAE, CVRMSE, and R^2 were calculated using Equations (1), (2), and (3), respectively:

$$\mathrm{MAE} = \frac{1}{n}\sum_{i=1}^{n}\left|x_a - y_p\right| \tag{1}$$

$$\mathrm{CVRMSE} = \frac{1}{\bar{x}}\sqrt{\frac{\sum_{i=0}^{n}\left(x_a - y_p\right)^2}{n}} \times 100\% \tag{2}$$

$$R^2 = 1 - \frac{\sum_{i=1}^{n}\left(Y_i - \overline{Y}\right)}{\sum_{i=1}^{n}\varepsilon_i{}^2} \tag{3}$$

where x_a is the real value, y_p is the predicted value, $\bar{x}$ is the mean of x_a, Y_i is the i-th dependent variable, $\overline{Y}$ is the mean of Y_i, and ε_i is the regression analysis error [63, 64].

2.2 | Development of the MPCA for the Indoor ERV System

2.2.1 | Development of the Rule-Based Control Algorithm

The rule-based algorithm developed in this study prioritized the control of PM levels in the control hierarchy, followed by CO_2 and temperature. The algorithm operated following Steps A to E within a single control cycle. The final system control value in the rule-based algorithm was determined based on the current IAQ conditions. When the ERV system was activated, the process entered Step A. In Step A, environmental data measured using sensors within the ERV system and the operational status were collected and stored in a real-time database. In Step B, additional variables, such as occupancy schedules and room schedules in spaces where the control algorithms were employed, were input alongside the environmental data from Step A. This was the initial decision-making phase that determined whether to activate the ventilation system and algorithm. The ERV system remained inactive on days without scheduled occupancy, such as weekends, holidays, or breaks, or during hours from the end of the school day until the start of the next. If the conditions for activation were met, the rule-based algorithm proceeded to Step D. This process is detailed in Figure 1.

In Step D, the decision-making phase determined the operational mode and airflow rate of the ERV system based on the indoor and outdoor PM concentrations, indoor CO_2 levels, and temperature. The primary criterion was the indoor $PM_{2.5}$ concentration. Although the School Health Act Enforcement Rules recommend maintaining indoor $PM_{2.5}$ levels below $35\,\mu g/m^3$, this algorithm set a lower threshold by referencing other standards. The first threshold was set at $15\,\mu g/m^3$, based on the "good" $PM_{2.5}$ concentration level defined by the Korean Ministry of Environment, and the second threshold was set at $25\,\mu g/m^3$ in accordance with World Health Organization (WHO) guidelines. Accordingly, indoor $PM_{2.5}$ levels were checked against the 15- and 25-$\mu g/m^3$ thresholds. If the indoor $PM_{2.5}$ concentration was $15\,\mu g/m^3$ or below, the IAQ was considered good and air purification was not activated. If the indoor $PM_{2.5}$ concentration exceeded $15\,\mu g/m^3$, either air purification or ventilation was initiated, with further criteria employed to determine the airflow rate. The choice between air purification and ventilation was based on a comparison of the indoor and outdoor $PM_{2.5}$ concentration; if the outdoor $PM_{2.5}$ concentration was higher than the indoor concentration, the air purifier operated in recirculation mode (air purification), whereas if the outdoor $PM_{2.5}$ concentration was lower than the indoor concentration, ventilation mode was activated to introduce outdoor air. If the indoor $PM_{2.5}$ concentration was $25\,\mu g/m^3$ or below, the system operated at a low airflow, but if it exceeded $25\,\mu g/m^3$, the indoor $PM_{2.5}$ concentration was considered severe, and the system was immediately set to a medium airflow for emergency operation.

The second criterion was to maintain the current CO_2 concentration at or below 1500 ppm. Standards for CO_2 concentrations vary widely by country, building, and purpose, with maximum levels up to 5000 ppm [65], and no clear international standard

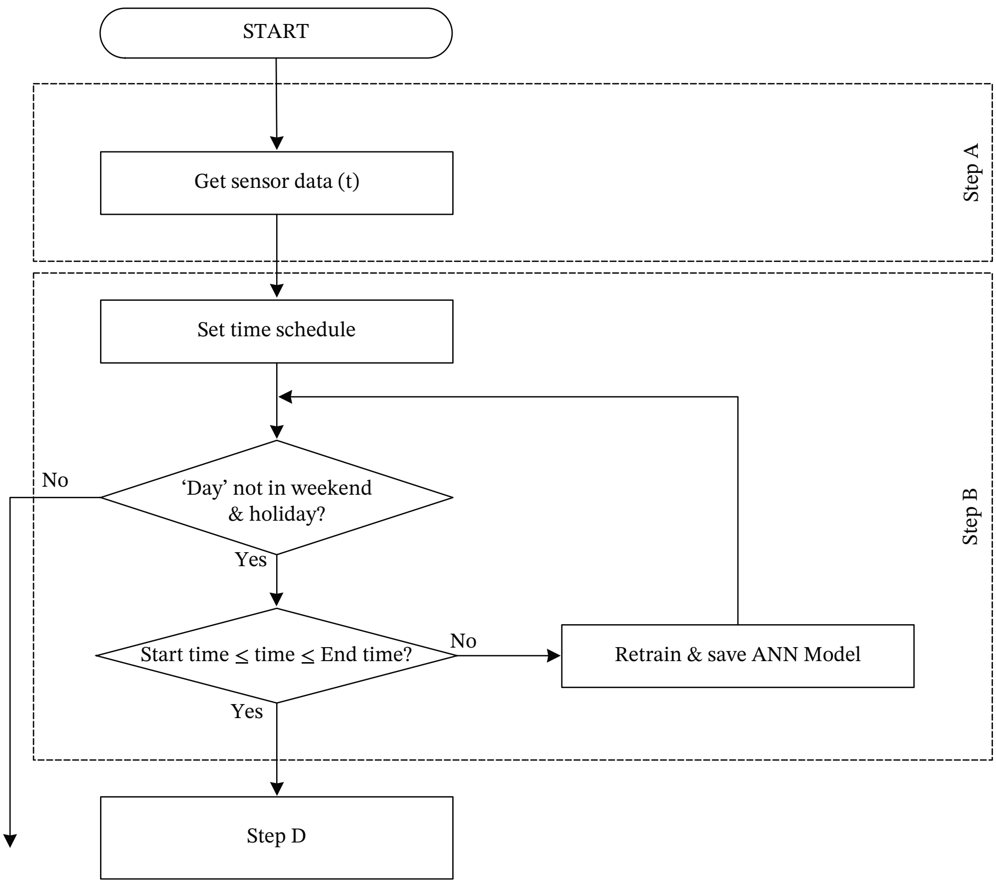

FIGURE 1 | Rule-based algorithm process.

exists. Therefore, this study adopted the 1500 ppm standard specified in the School Health Act Enforcement Rules, the most clearly established standard. Given that CO_2 can have more immediate adverse effects on occupants than $PM_{2.5}$ and can be quickly reduced in ventilation mode, the system was configured to prioritize control if the real-time CO_2 concentration rose above 1500 ppm, selecting the outdoor air intake mode ahead of the first criterion. The third criterion was the current indoor temperature. If the current indoor temperature was between 18°C and 28°C, the indoor thermal environment was considered comfortable.

When the decision-making process was completed in Step D, Step E was initiated, commanding the system to operate according to the optimal control solution derived in the previous step. At this point, the operating mode and airflow rate of the ERV system were set to the values determined in Step D. The operation cycle was then repeated after completing all of these steps. Steps D and E are summarized in Figure 2.

2.2.2 | Development of the MPCA Containing the Prediction Models

The MPCA added the prediction models for the indoor $PM_{2.5}$ concentration, CO_2 concentration, and temperature 5 min ahead to the previously developed rule-based algorithm. The overall structure of the MPCA was identical to that of the rule-based algorithm but with the inclusion of Step C. In this step, the real-time data collected in Step A were used to retrain the prediction models and to generate predictions for each control factor. Retraining was scheduled to occur once every Friday, but it would only occur if at least 510 data points (equivalent to a minimum of 1 day's IAQ data) meeting the training data selection criteria had accumulated. For predictions, the airflow rate of the ventilation system was used as an input variable along with the current indoor environmental parameters, enabling the algorithm to determine the lowest airflow rate that could maintain the indoor $PM_{2.5}$ concentration, CO_2 concentration, and temperature at the appropriate levels with minimal energy consumption.

The predicted values were then utilized in Step D as a substitute for the current $PM_{2.5}$ concentration, CO_2 concentration, and temperature to make decisions, thus enabling preemptive IAQ control. At this stage, the airflow rate output from Step C was directly employed, whereas only the mode decision was handled separately before proceeding to Step E. In the conventional rule-based control strategy, the ventilation system was activated only when the indoor $PM_{2.5}$ concentration exceeded the threshold. However, with the MPCA, the ERV system was preemptively activated to reduce the indoor $PM_{2.5}$ concentration before it surpassed the threshold. Preemptive control of the ERV system in accordance with the predicted $PM_{2.5}$ values is illustrated in Figure 3. The same principle was applied to the indoor CO_2 concentration, allowing the MPCA to maintain the CO_2 concentrations beneath the threshold for a longer period. The structure of Step C in the MPCA is detailed in Figure 4, whereas Steps D to E for the MPCA are summarized in Figure 5.

2.3 | Establishment of the Living Lab and Empirical Experiments

2.3.1 | Details of the Living Lab

A living lab is a combined lab-household system designed for the development of integrated technical innovations [66]. Living labs can be deployed in real-life situations or devised using simulations; in the present study, an actual school facility currently in use was selected. The spaces chosen as the location for the living lab were remodeled first-grade classrooms in an elementary school located in Uijeongbu, Gyeonggi-do, Korea, where architectural and mechanical improvements had previously been made. According to the Köppen–Geiger classification system, Uijeongbu has a continental monsoon climate (Dwa), with an annual average temperature of approximately 11.5°C. The monthly annual average temperature

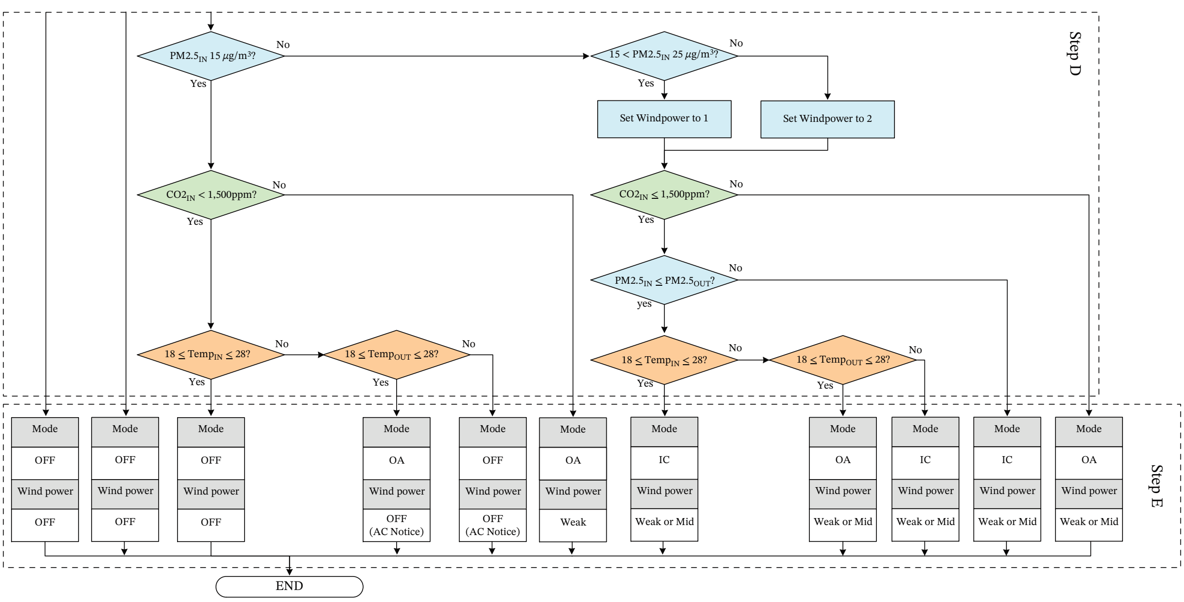

FIGURE 2 | Steps D and E of the rule-based algorithm.

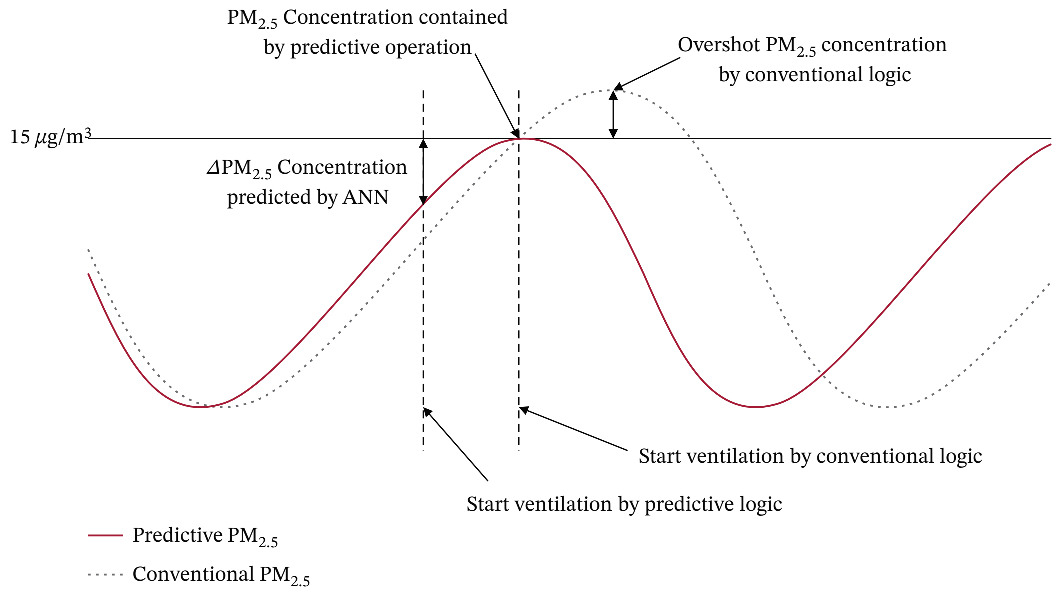

FIGURE 3 | Concept diagram for preemptive control in accordance with the predicted PM2.5 concentration.

ranges from −2.1°C in January to 25.7°C in August, whereas the monthly annual average RH varies from 59% in March to 78% in July. The annual average precipitation is approximately 1300 mm, with much of this concentrated in summer (June–August). The monthly annual $PM_{2.5}$ concentration ranges from 14 μg/m^3 in August to 35 μg/m^3 in March. In summer, the $PM_{2.5}$ concentration is lower because of the higher precipitation, whereas in February and March, the $PM_{2.5}$ concentration increases because of the yellow dust arriving from China. The monthly annual CO_2 concentration ranges from 403 ppm in August to 420 ppm in January. During the 1st semester from March to July, the average temperature and humidity rise, whereas during the 2nd semester from September to December, the average temperature and humidity decrease. The opposite trends are observed for the $PM_{2.5}$ and CO_2 concentrations.

The school building used in the present study was representative of a standard elementary school building in South Korea, with a total floor area of 10,913 m^2, four floors, and 26 classrooms accommodating approximately 20 students and one teacher per class. This facility achieved a 29% reduction in PM infiltration by installing airtight windows, air curtains, and dust-absorbing mats at the main entrances [67]. Three first-grade classrooms on the first floor of the building were equipped with window-type outdoor-air-intake ERV systems, and the doors and windows had been upgraded, ensuring the airtight performance needed for experimentation, thus qualifying them as a suitable living lab.

In this study, the classrooms used in the living lab had been subject to identical mechanical and facility improvements, had the same occupancy per classroom, and followed the same basic academic schedule. Each classroom was equipped with real-time monitoring sensors to collect data from the window-type ventilation system. Details of the classrooms are presented in Table 4.

The ventilation system installed in the classrooms was an outdoor air-intake ERV system mounted at the top of the windows. This system was pre-set to operate in air purification mode, which employed forced ventilation of approximately 60 m^3 within 10–15 min. It also offered four additional modes—outdoor air intake, indoor air recirculation, purification, and bypass—and three adjustable airflow levels (high, medium, and low). The internal components of the ventilation unit included two fans, three damper motors, a heat exchanger, and filters to provide ventilation and air purification functions. The fans were located on the intake and exhaust sides of the system, with a HEPA filter attached to the intake bringing in outdoor air and a prefilter on the exhaust side for discharged indoor air. HEPA filters can capture up to 99.97% of external PM and IAQ contaminants when outdoor air is introduced.

This ventilation system was equipped with an indoor air recirculation function and could independently purify air using its built-in HEPA filter, distinguishing it from conventional ERV systems. The indoor air recirculation mode operates one fan to recirculate indoor air without utilizing outdoor air at all, whereas the outdoor air intake mode operates two fans, one to supply and one to remove air, with the outdoor air moving through the filter when let in. Both modes have the air go through the HEPA filter as part of the air purification process. Therefore, this study refers to the equipment as the outdoor air-intake ERV system or simply the ERV system. When there were no occupants in the classroom, the ERV system ceased operation and was switched to a powered-off state.

The ERV system was equipped with precalibrated sensors installed by the manufacturer and selected service provider. These sensors provided continuous real-time measurements during the empirical experiment. All sensors were factory-calibrated prior to installation. Details of the ERV system and specifications of the sensors installed in the classrooms are provided in Table 5.

2.3.2 | Data Collected From the Living Lab and Empirical Experiments

In this study, the IAQ improvement and energy consumption of the MPCA and the rule-based algorithm were evaluated in real time under actual occupancy conditions. A total of

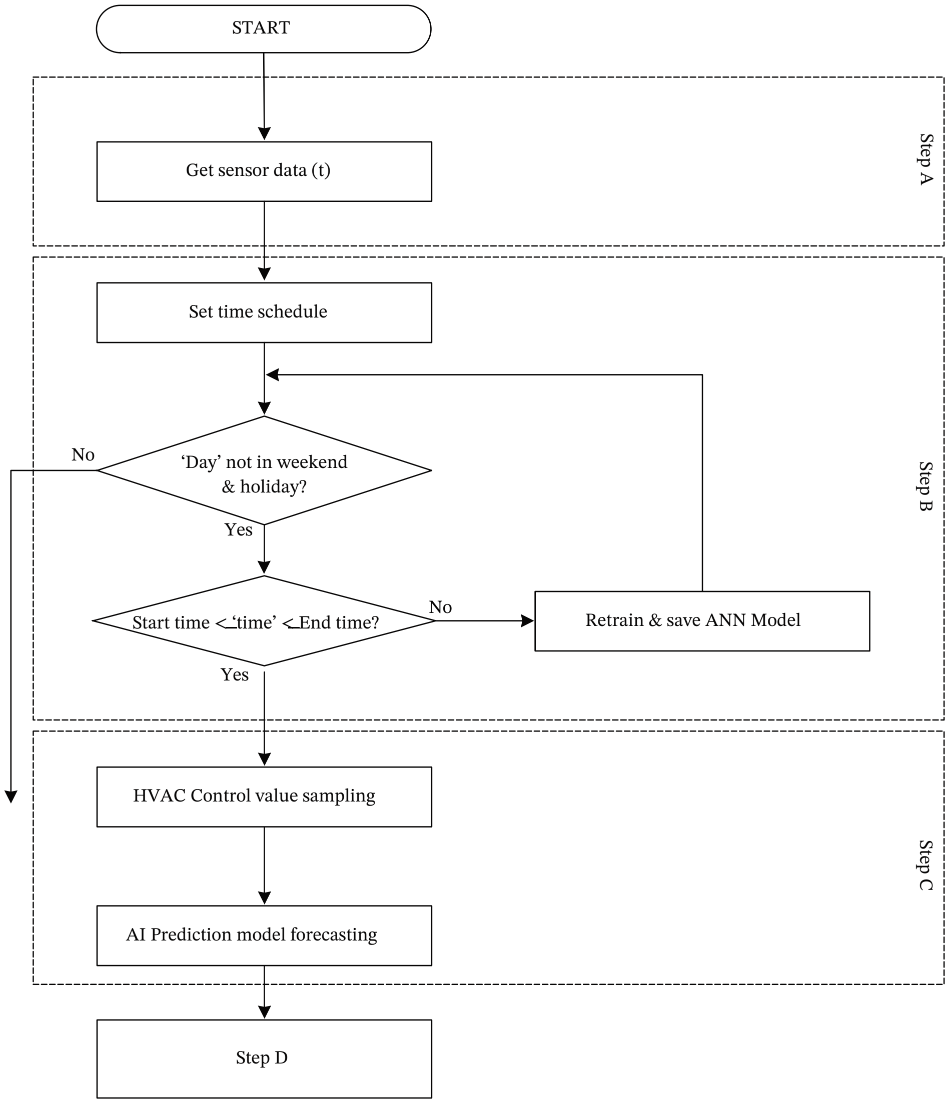

FIGURE 4 | MPCA process (Steps A–C).

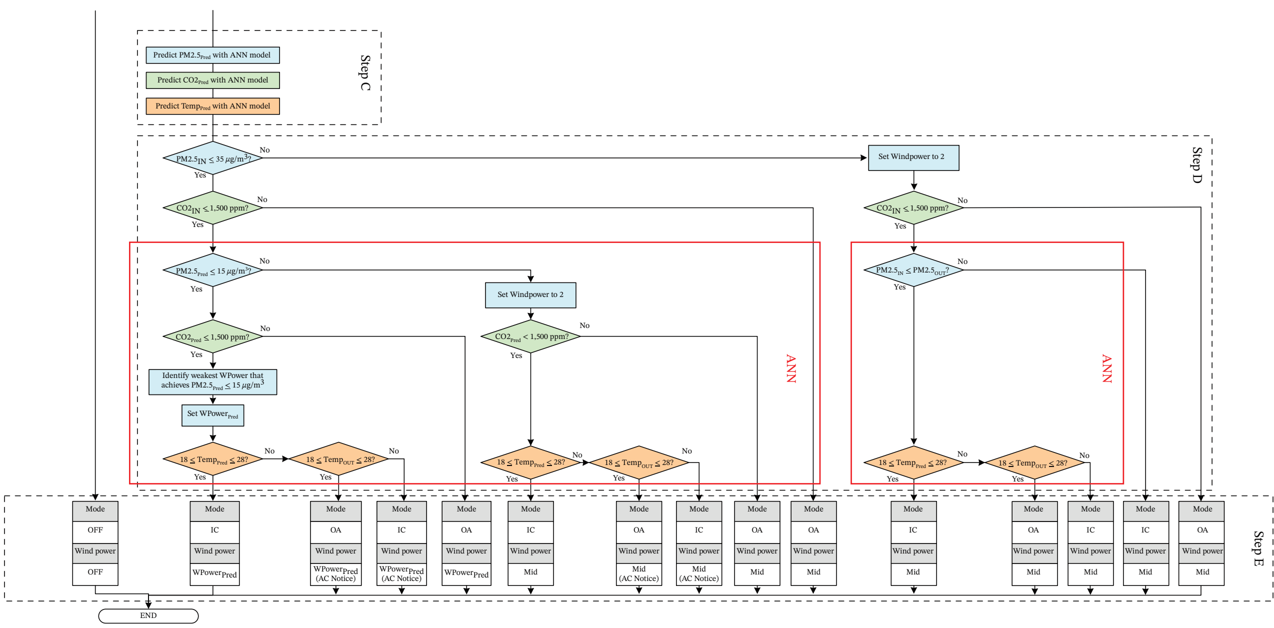

FIGURE 5 | MPCA process (Steps C–E).

TABLE 4 | Living lab details.

		Details
Building information	Location	Uijeongbu-si, Gyeonggi-do, Republic of Korea
	Size	$11 \times 8 \times 3$ m ($W \times D \times H$)
	Floor	1F
	Selected for the living lab	Three first-grade classrooms
Occupant information	Occupancy	A total of 1 teacher and 20 or 21 first-grade students in each classroom
	Occupant hours	Weekdays
		08:00–09:00: Teacher only present
		09:00–14:30: Teacher and students present.
		14:30–16:30: Teacher and a minimal number of students are present
	Unoccupied hours	Weekends, holidays, and after 16:30 p.m.–before 8 a.m.
Building plan and living lab images		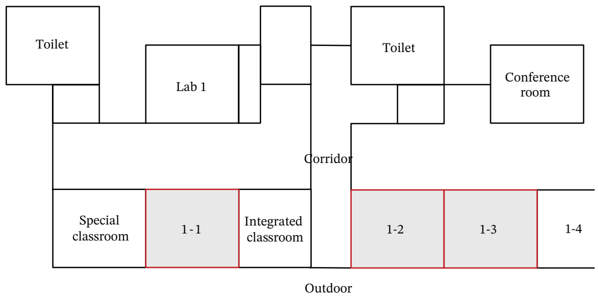 

6 days of empirical testing was conducted for this purpose. The experiment was conducted in the three active living-lab classrooms. Class A employed the MPCA, Class B ran the ERV system autonomously under occupant discretionary control (ODC) without an algorithm, and Class C used the rule-based algorithm. In Class B, the teacher continuously operated the ERV system in automatic mode with low airflow throughout the experiment. All three classes were instructed not to manually open the windows or doors for ventilation, except when the students entered or exited.

To evaluate the statistical significance of differences among the three control strategies (MPCA, rule-based control, and ODC), daily mean values of $PM_{2.5}$ and CO2 were analyzed using one-way ANOVA. ANOVA is a statistical analysis used for comparing mean values of three or more groups, and since this experiment operates three different control strategies (MPCA, rule-based, and ODC), we decided ANOVA comparison is suitable. After ANOVA comparison, Tukey's HSD post hoc tests were conducted for pairwise comparisons. Additionally, standard deviations (SD) and 95% confidence intervals (CI) were calculated to quantify variability and test statistical robustness. Apart from daily mean values' comparison, other statistical comparisons were conducted to support each control algorithms' performance results in class hours specifically, and for relative comparison of energy consumptions. All analyses were performed using Python (SciPy and Statsmodels).

Schedules were collected to exclude data on days with outdoor activities or nonschool days. Data were collected from October 10 to October 23, 2023, focusing on 6 days where all three classes remained indoors with no special activities, thus allowing for real-time data collection and comparative analysis. The selected experiment days were in October during the autumn semester because the spring semester has a relatively unstable academic schedule due to regular outdoor activities or events and has a potential risk of extreme outlier incidents originating from

TABLE 5 | Ventilating purifier details.

	Details	
Device image		
Device layout and ventilation route	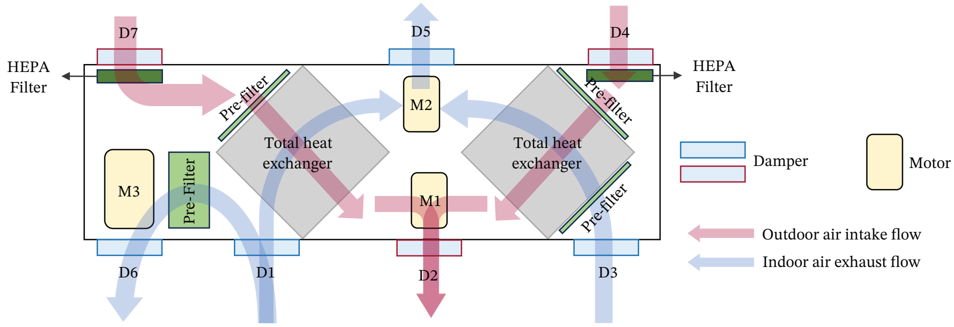	
Device specifications	Ventilation fan motor	Fans 1and 2 (2 in total)
	Damper motor	Dampers 1, 2, and 3 (3 in total)
	Sensors	CO_2 sensors
		$PM_{2.5}$ sensors
		Indoor/outdoor temperature/ humidity sensors
	Remote control	RF receiver for transmitter (remote control)
Device mode and supply air power	Operation mode	Indoor air circulation, outdoor air supply, and auto (not used in the study)
	Supply air power	Low: 150 CMH
		Middle: 250 CMH
		High: 400 CMH
Specifics	Attached to the upper window, heat exchanger and HEPA filter installed	
Sensor Specifics	PM2.5: Range 0–500 $\mu g/m^3$, resolution 1 $\mu g/m^3$, and maximum error ± 10% at 100–500 $\mu g/m^3$	
	CO2: NDIR dual-wavelength, range 0–3000 ppm, accuracy ± 2%FS or ± 3% of reading, update interval 2 s	
	Temperature: accuracy ± 0.2°C (0°C–65°C), ± 2% RH, and response time 8–86 s	

yellow dust, which can disrupt the experimental conditions. Additionally, winter and summer have not been selected as experiment periods, because even though they possess the most extreme outdoor conditions suitable for empirical experiments, they have winter and summer school breaks and thus have less school schedules for experiment to be implemented or have significant impact.

3 | Results

3.1 | Performance Evaluation of the Prediction Models Before and After Retraining

The retraining performance of the prediction models for the $PM_{2.5}$ concentration, CO_2 concentration, and indoor temperature was assessed using data from the living lab that was not included in the training dataset. The predictive performance of each model is summarized in Table 6 and Figure 6. Of the three prediction models, the $PM_{2.5}$ model had the lowest predictive performance, likely because $PM_{2.5}$ is more readily influenced by environmental factors, and its concentration is thus more difficult to track accurately. Prior to retraining, the $PM_{2.5}$ model had a CVRMSE of 34.83%, exceeding the ASHRAE-recommended threshold of 30% for hourly data [27]. However, after retraining, the $PM_{2.5}$ model produced a CVRMSE of 27.10%, representing a 22% improvement and meeting ASHRAE standards, while the R^2 value also improved from 0.79 to 0.90, a 14% improvement. The CO_2 and temperature prediction models also demonstrated improved prediction performance after retraining. The CO_2 model improved by 7% in terms of the CVRMSE and 1% in its R^2 value, whereas the temperature model produced improvements of 22% for the CVRMSE and 34% for R [2].

3.2 | Empirical Results and Analysis From the Living Lab

3.2.1 | Air Quality Improvement

To assess the improvement in the air quality when using each algorithm, the daily average $PM_{2.5}$ and CO_2 concentrations, average IAQ over the entire experimental period, average IAQ by occupant activity, and the duration of time the IAQ remained within a previously set threshold were analyzed. The daily average $PM_{2.5}$ and CO_2 concentrations for each classroom during occupant hours over a 6-day period are presented in Table 7 and Figure 7. The results indicate that the classrooms with the MPCA (Class A), ODC (Class B), and the rule-based algorithm (Class C) maintained average $PM_{2.5}$ and CO_2 concentrations within acceptable thresholds, with the ODC classroom producing the highest IAQ. Between the two classrooms operated using a control algorithm, the MPCA classroom maintained a higher

TABLE 6 | Performance of the prediction models before and after retraining.

		Evaluation criteria		
		MAE	CVRMSE	R^2
$PM_{2.5}$	Before	2.54	34.83	0.79
	After	2.13 (0.41 ▼)	27.10 (7.73 ▼)	0.90 (0.11 ▲)
CO_2	Before	70.51	11.49	0.98
	After	23.38 (47.13 ▼)	3.34 (8.15 ▼)	0.99 (0.01 ▲)
Temp.	Before	0.93	4.70	0.61
	After	0.65 (0.28 ▼)	3.66 (1.04 ▼)	0.82 (0.21 ▲)

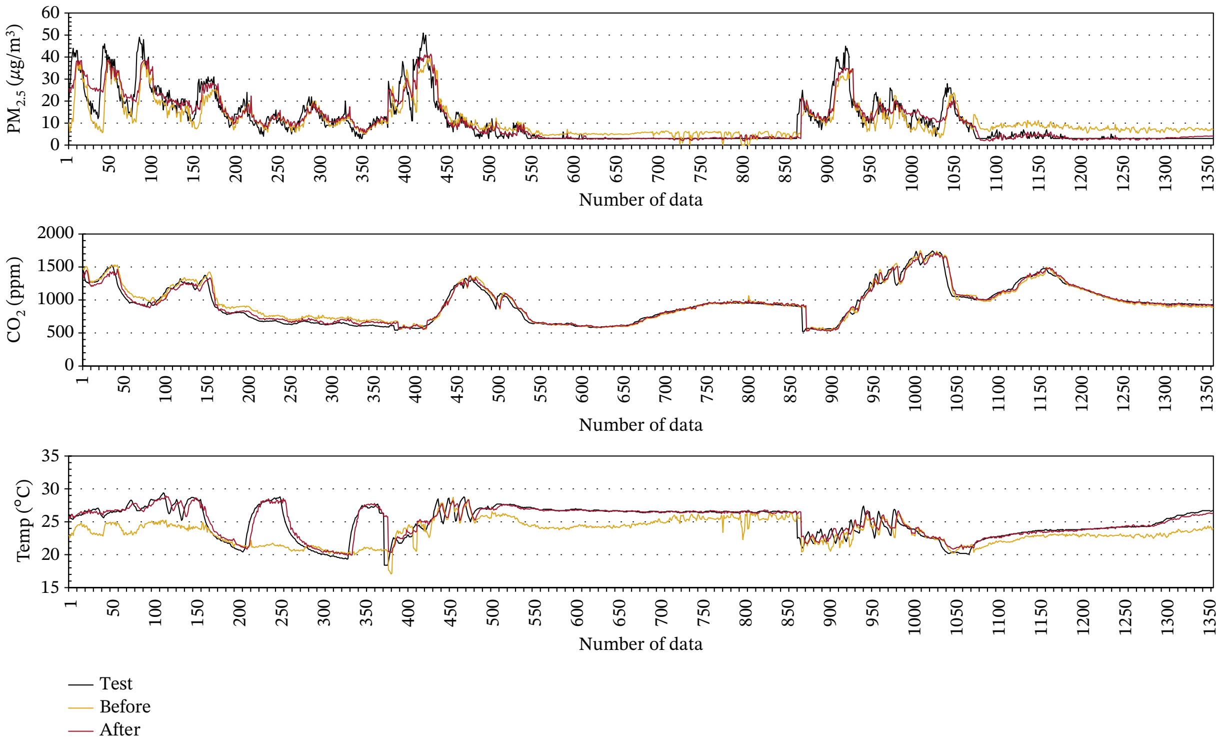

FIGURE 6 | Comparison of test data and prediction before and after retraining for each input.

TABLE 7 | Daily average $PM_{2.5}$ and CO_2 concentrations by control method.

	MPCA		ODC		Rule-based control	
	$PM_{2.5}$ ($\mu g/m^3$)	CO_2 (ppm)	$PM_{2.5}$ ($\mu g/m^3$)	CO_2 (ppm)	$PM_{2.5}$ ($\mu g/m^3$)	CO_2 (ppm)
Day 1	7.91	1194.29	5.24	936.09	10.59	1165.11
Day 2	10.28	940.23	3.94	794.58	12.38	935.28
Day 3	10.69	890.44	4.00	901.46	14.33	1063.01
Day 4	9.57	843.79	5.28	852.99	14.39	1041.07
Day 5	14.64	975.24	5.76	867.82	15.25	1031.67
Day 6	8.17	1195.54	10.81	1068.48	10.50	1227.86
Overall average	10.21	1006.59	5.84	903.57	12.91	1077.33

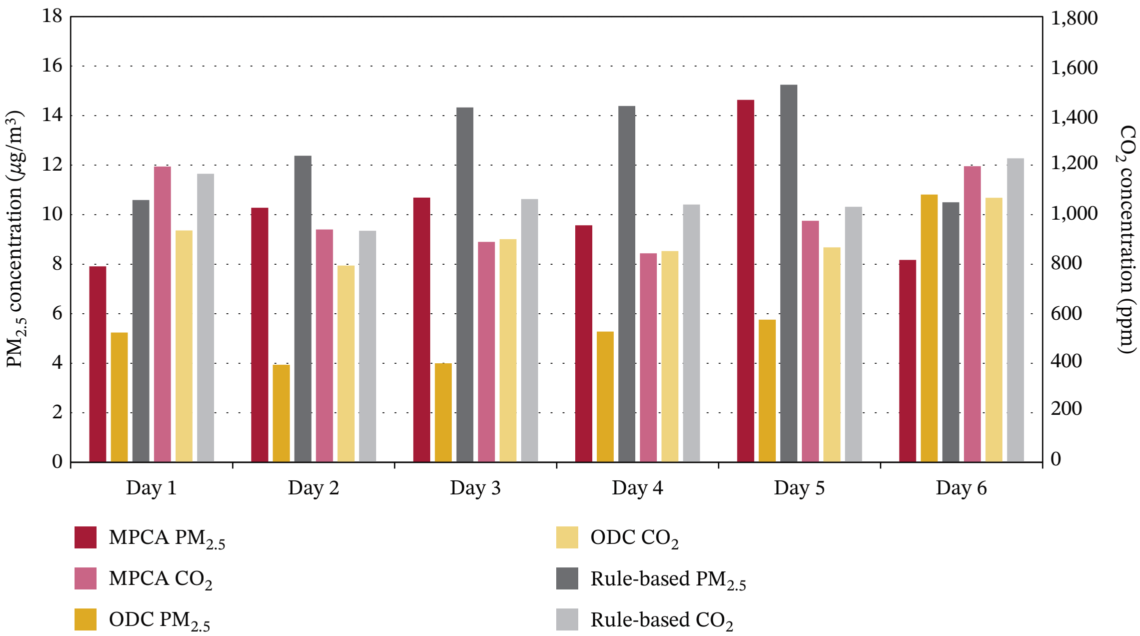

FIGURE 7 | Visualization of daily average $PM_{2.5}$ and CO_2 concentrations by control method.

average air quality than the rule-based control classroom. In terms of the average IAQ across the entire period, the use of the MPCA led to an approximately 21% lower $PM_{2.5}$ concentration and 7% lower CO_2 concentration than with rule-based control.

Statistical analysis of the daily mean values has been conducted to evaluate the statistical significance. For $PM_{2.5}$, mean value, SD, and 95% CI of each algorithm are as follows; MPCA showed mean value of 10.21 with SD of 2.44 and 95% CI of 7.65 to 12.77. ODC showed mean value of 5.84 with SD of 2.54 and 95% CI of 3.17 to 8.51. Rule-based control showed mean value of 12.91 with SD of 2.06 and 95% CI of 10.75 to 15.07. Therefore, the ANOVA for $PM_{2.5}$ revealed significant differences among the three strategies ($F = 13.76$, p value < 0.001). Tukey's HSD confirmed that rule-based control maintained significantly higher concentrations than both MPCA and ODC, whereas MPCA was higher than ODC, though this was due to excessive use of the ventilation system in ODC classroom. For CO_2, mean value, SD, and 95% CI of each algorithm are as follows; MPCA showed mean value of 1006.59 with SD of 152.52 and 95% CI of 846.53–1166.65. ODC showed mean value of 903.57 with SD of 93.78 and 95% CI of 805.15–1001.99. Rule-based control showed mean value of 1077.33 with SD of 104.06 and 95% CI of 968.12–1186.54. In case of CO_2, differences did not reach statistical significance ($F = 3.20$, $p = 0.069$) in comparison with that of $PM_{2.5}$. Nevertheless, MPCA consistently showed lower CO2 levels than rule-based control across all 6 days, with reductions of 3%–13%.

The average IAQ based on the $PM_{2.5}$ and CO_2 concentrations and the time spent under the acceptable threshold by activity type are summarized in Table 8. Occupant activities were broadly categorized into class hours and nonclass hours (including arrival, dismissal, homeroom, breaks, lunch, etc.). MPCA showed 40% lower $PM_{2.5}$ concentrations during class hours and 10.5% lower $PM_{2.5}$ concentrations during nonclass hours in comparison with rule-based control. Also, MPCA showed 3% lower CO_2 concentrations during class hours and 13.4% lower CO_2 concentrations during nonclass hours in comparison with rule-based control.

The length of time for which the $PM_{2.5}$ concentration remained at or below 15 $\mu g/m^3$ and the CO_2 concentration remained at or below 1500 ppm was also calculated. The analysis revealed that

TABLE 8 | Average $PM_{2.5}$ and CO_2 concentrations and time under the threshold by control method and class activity.

			MPCA	ODC	Rule-based control
$PM_{2.5}$	Average concentration ($\mu g/m^3$)	Class hours	7.65	4.18	12.73
		Nonclass hours	11.53	6.77	12.89
	Total time under 15 $\mu g/m^3$ (min)	Class hours	885	775	610
		Nonclass hours	1245	1766	1402
CO_2	Average concentration (ppm)	Class hours	1395.63	1114.48	1439.69
		Nonclass hours	796.36	792.36	919.46
	Total time under 1500 ppm (min)	Class hours	576	775	446
		Nonclass hours	1700	1925	1677

ODC maintained a suitable IAQ for the longest period, followed by MPCA and rule-based control. For the indoor $PM_{2.5}$ concentration, the total duration under the threshold was 2130 min for MPCA, 2541 min for ODC, and 2012 min for rule-based control, with an average daily time under the threshold of 355.00, 423.50, and 335.33 min, respectively. For the indoor CO_2 concentration, the total time under the threshold was 2276 min for MPCA, 2700 min for ODC, and 2029 min for rule-based control, with a daily average of 379.33, 450.00, and 338.17 min, respectively. Notably, the CO_2 concentration never exceeded 1500 ppm under ODC because the ERV system operated continuously in outdoor air-intake mode.

As a result, the MPCA maintained lower levels of $PM_{2.5}$ and CO_2 for a longer time than the rule-based algorithm. Notably, during class hours, the MPCA achieved 885 min of lower $PM_{2.5}$ levels and 576 min of lower CO_2 levels, representing improvements of 45% and 29%, respectively, compared with the rule-based algorithm.

TABLE 9 | Airflow rate and power consumption for the outdoor air-intake ERV system by operation mode.

		Airflow rate (CMH)	Power consumption (W)
SA	High	166.8	36.8
	Middle	131.4	24.2
	Low	105.0	16.7
EA	High	165.0	36.8
	Middle	130.2	24.2
	Low	106.8	16.7
Purification/ bypass	High	166.2	27.9
	Middle	132.0	17.6
	Low	103.2	12.3

3.2.2 | Energy Consumption According to the Control Method

Overall, all three control strategies proved capable of maintaining the IAQ under the required thresholds. However, the development of optimal control algorithms that can improve both the IAQ and energy efficiency is also an important goal. Some recent studies have employed multiobjective optimization strategies for this purpose but have not demonstrated their practical application in school environments [68, 69]. Therefore, in the present study, the energy consumption for each algorithm was analyzed based on the hourly power consumption of the outdoor air-intake ERV system under different operating modes and airflow rates (Table 9). Due to the structure of the ERV system, energy consumption almost doubled when operating in outdoor air-intake mode (i.e., with the fans for supplying air [SA] and exhausting air [EA] both active) compared with indoor air-recirculation mode, during which only the purification fan was active.

To compare the energy consumption between the control methods, the total hourly energy consumption, energy consumption by occupant activity type, and energy consumption during periods of acceptable IAQ were all determined. The operating hours and energy consumption for each living-lab classroom are presented in Table 10 and Figure 8. The following combinations were analyzed: outdoor air intake mode + medium airflow rate (OutMid), outdoor air intake mode + low airflow rate (OutLow), indoor air circulation mode + medium airflow rate (InMid), and indoor air circulation mode + low airflow rate (InLow).

The operating hours were highest for ODC, followed by MPCA and rule-based control. However, although the total energy consumption was also highest for ODC (1346.83 W), rule-based control had a higher energy consumption than MPCA (571.85 and 539.51 W, respectively). Thus, ODC resulted in approximately 2.4–2.5 times higher energy consumption compared with algorithm-controlled operation.

The MPCA operated in outdoor air-intake mode for 585 min and in recirculation mode for 809 min, whereas the rule-based algorithm operated in outdoor air-intake mode for 834 min and recirculation mode for 502 min. Thus, despite the longer overall operating time, the MPCA reduced outdoor air intake and increased recirculation. As a result, the energy consumption was 334.6 W for outdoor air intake and 204.9 W for recirculation, compared with 464.5 and 107.4 W, respectively, for the rule-based algorithm.

TABLE 10 | Operating hours and energy consumption according to the control method by mode and airflow rate.

		Operating hours (min)		Energy consumption (W)	
MPCA	IA/low	365	1394	74.83	539.51
	IA/mid	444		130.09	
	OA/low	550		306.35	
	OA/mid	35		28.25	
ODC	Auto/low (OA/low)	2418		1346.83	
Rule-based control	IA/low	452	1336	92.66	571.85
	IA/mid	50		14.65	
	OA/low	834		464.54	
	OA/mid	0		0	

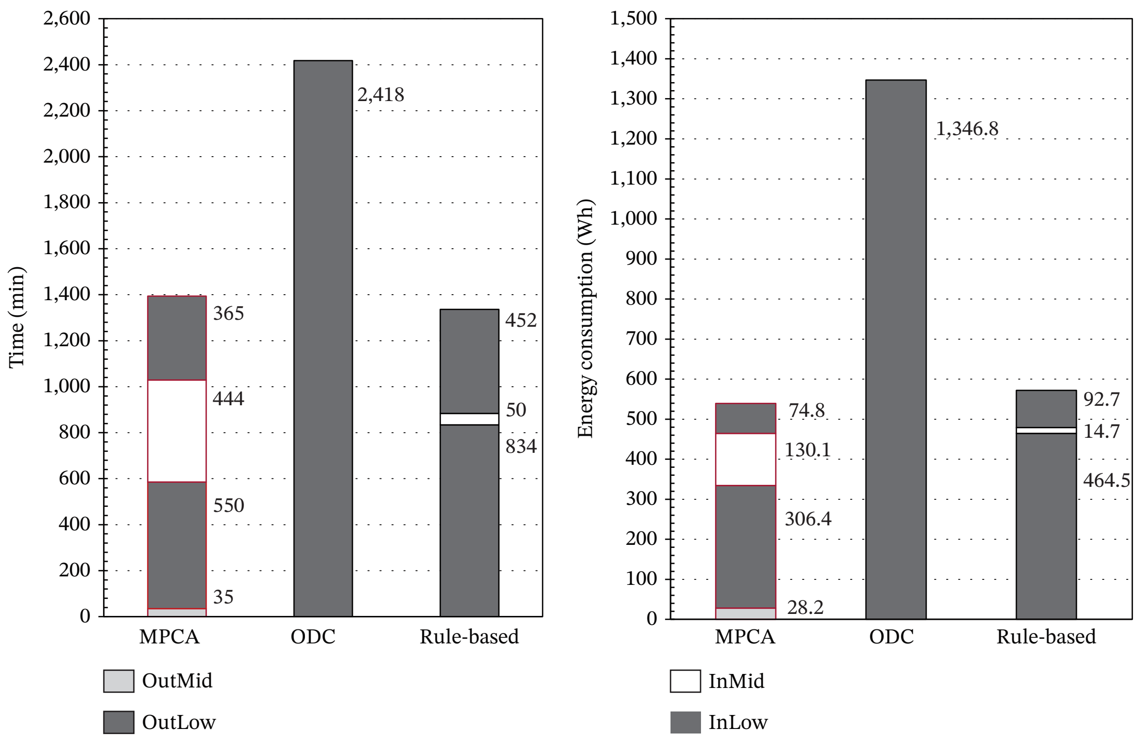

FIGURE 8 | Visualization of operating hours and energy consumption by the control method by mode and airflow rate.

A comparative analysis of the operating time and energy consumption by occupant activity type was also conducted (Table 11 and Figure 9). Under the MPCA during class hours, indoor air recirculation under medium airflow was the most common operation mode, followed by indoor air recirculation under low airflow, outdoor air intake under medium airflow, and outdoor air intake under low airflow. During nonclass hours, the order changed to outdoor air intake under low airflow, indoor air recirculation under low airflow, indoor air recirculation under medium airflow, and outdoor air intake under medium airflow. As for energy consumption, the outdoor air intake mode under low airflow had the second-highest energy consumption, whereas outdoor air intake mode under medium airflow had the third-highest and indoor air recirculation under low airflow had the lowest energy use. This discrepancy between energy consumption and operating hours was due to the more energy-intensive nature of outdoor air intake compared with indoor air recirculation.

On the other hand, under the rule-based algorithm during both class and nonclass hours, outdoor air intake under low airflow was the most common operational mode, followed by indoor air recirculation under low airflow and indoor air recirculation under medium airflow.

The energy consumption during periods when indoor contaminant concentrations remained below the acceptable thresholds despite continuous operation of the ventilation system is presented in Figure 10, illustrating the degree to which the two algorithms avoided unnecessary operation. ODC was excluded from this analysis because the system operated continuously, leading to excessive energy use.

TABLE 11 | Operating hours and energy consumption by occupant activity.

		Class hours		Nonclass hours	
		Operating hours (min)	Energy consumption (W)	Operating hours (min)	Energy consumption (W)
MPCA	IA/low	76	15.58	289	59.25
	IA/mid	305	89.37	139	40.73
	OA/low	29	16.15	521	290.20
	OA/mid	33	26.63	2	1.61
Rule-based control	IA/low	102	20.91	350	71.75
	IA/mid	8	2.34	42	12.31
	OA/low	412	229.48	422	235.05
	OA/mid	0	0	0	0

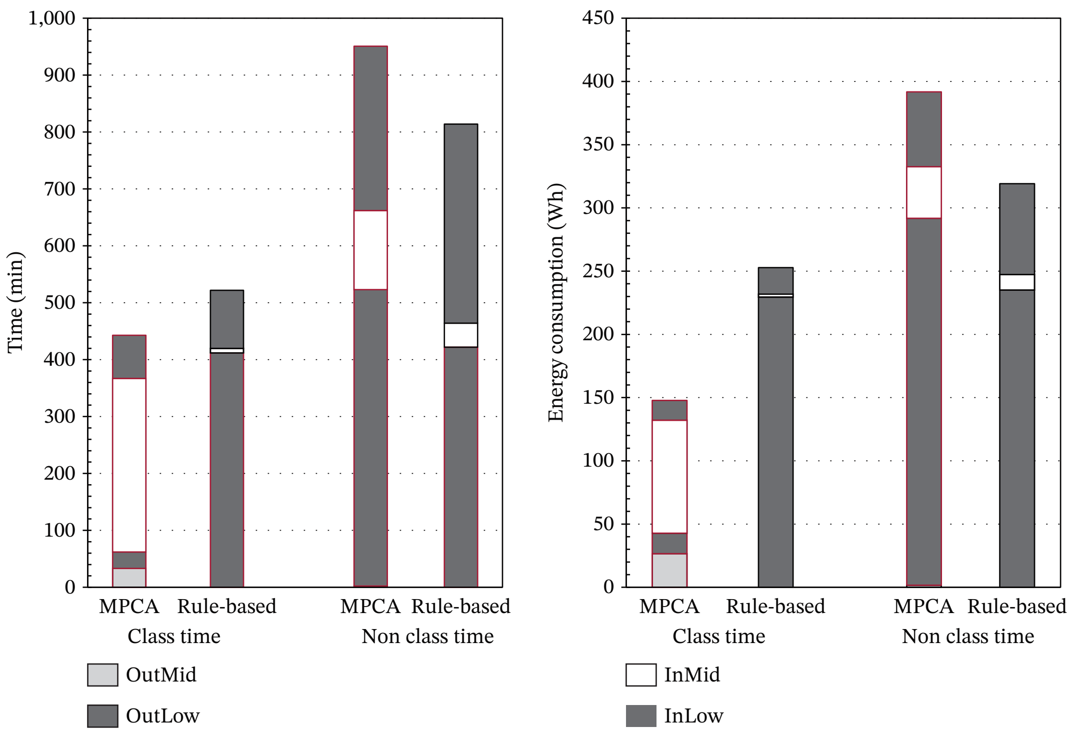

FIGURE 9 | Operating hours and energy consumption by algorithm and classroom activity.

Under the MPCA, the energy consumption was 932 W when the $PM_{2.5}$ concentration was below 15 $\mu g/m^3$, 1117 W when the CO_2 concentration was below 1500 ppm, and 658 W when both $PM_{2.5}$ and CO_2 were within a normal range. In contrast, for the rule-based algorithm, the energy consumption was 919, 945, and 563 W, respectively.

During periods when the contaminants were below the threshold, the MPCA maintained lower $PM_{2.5}$ and CO_2 concentrations for a longer duration than the rule-based algorithm. Under the MPCA, the average $PM_{2.5}$ concentration was maintained at 10.64 $\mu g/m^3$ and the average CO_2 concentration at 974.80 ppm, with a total of 668 min of operation beneath the thresholds. In contrast, the rule-based algorithm maintained an average $PM_{2.5}$ concentration of 13.21 $\mu g/m^3$ and an average CO_2 concentration of 1065.22 ppm, with a time under the threshold of 563 min. Details of the average air quality during the periods where the $PM_{2.5}$ and CO_2 were under the threshold for each algorithm are presented in Table 12, and the overall $PM_{2.5}$ and CO_2 concentrations are summarized in Figure 11.

4 | Discussion

4.1 | Discussion on Performance Evaluation of the Prediction Models

After retraining, the prediction models exhibited improved performance across all metrics compared with before retraining. The prediction trends for each model before and after retraining

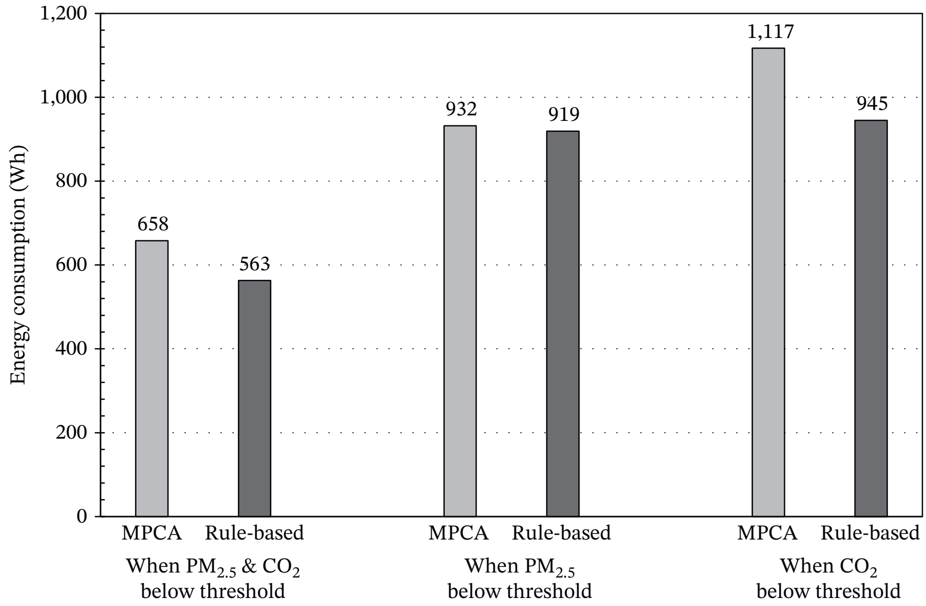

FIGURE 10 | Energy consumption during periods when the IAQ met the established threshold according to the control algorithm.

TABLE 12 | Average air quality using control algorithms during periods when the $PM_{2.5}$ and CO_2 concentrations were below the threshold.

	MPCA	Rule-based control
Average $PM_{2.5}$ concentration ($\mu g/m^3$)	10.64	13.21
Average CO_2 concentration (ppm)	974.80	1065.22
Operating hours beneath the threshold (min)	668	563

are presented in figure within Table 6, demonstrating how the models after retraining more closely tracked the true values. This was particularly clear for the temperature model, where abrupt fluctuations that were previously untracked were accurately tracked after retraining. This improved accuracy was likely due to the use of both recent data and data specifically tailored to reflect dynamic IAQ patterns during retraining.

Overall, the results demonstrated that the retraining process enabled the prediction models to adapt to an ever-changing environment, confirming that retraining could improve their prediction performance. Consequently, the retrained models were incorporated into the MPCA used in the living-lab experiment, with periodic retraining employed to ensure continuous improvement in the prediction accuracy. As described in Section 2.2.2, the retraining process for the algorithm was scheduled to occur once every Friday, but it would only occur if at least 510 data points meeting the same training data selection criteria used for model development had accumulated. The threshold of 510 data points was selected because this was equivalent to a minimum of 1 day's worth of acquired IAQ data. This would ensure at least one retraining cycle each week during regular semesters to adapt to changes in the weather, while avoiding excessive or unnecessary retraining during semester breaks. The retraining process took an average of 3–4 min and was set to operate outside of regular operation periods to avoid interfering with the automated control.

4.2 | Discussion on Empirical Results and Analysis From the Living Lab Experiment

4.2.1 | Discussions on Air Quality Improvement Analysis

The results of empirical experiment indicating that the classroom with the ODC produced the highest IAQ is thought to have been because of the ODC's discretionary nature. The teacher in charge of ventilation system operation kept the system running constantly which led to excessive, yet powerful ventilation. Between the two classrooms operated using a control algorithm, the MPCA classroom maintained a higher average air quality than the rule-based control classroom. Notably, despite the additional CO_2 introduced during two postschool meetings in the MPCA classroom on the first two experiment days, the average CO_2 concentration over the entire period was still lower in this classroom than in that with rule-based control, demonstrating the superior IAQ performance of the MPCA.

Although CO_2 differences were not statistically significant, the consistent downward trend under MPCA compared with rule-based control remains practically meaningful in classrooms where CO_2 frequently approaches regulatory thresholds. The lack of statistical significance is likely due to the small sample size ($n = 6$) and high day-to-day variability, whereas the more volatile characteristics of CO_2 in comparison with $PM_{2.5}$ could have also contributed to this end. Future studies with longer monitoring periods are needed to increase statistical power.

The results of average $PM_{2.5}$ and CO_2 concentrations by activity type analysis in accordance with Table 8 show that the MPCA maintained lower $PM_{2.5}$ and CO_2 concentrations than

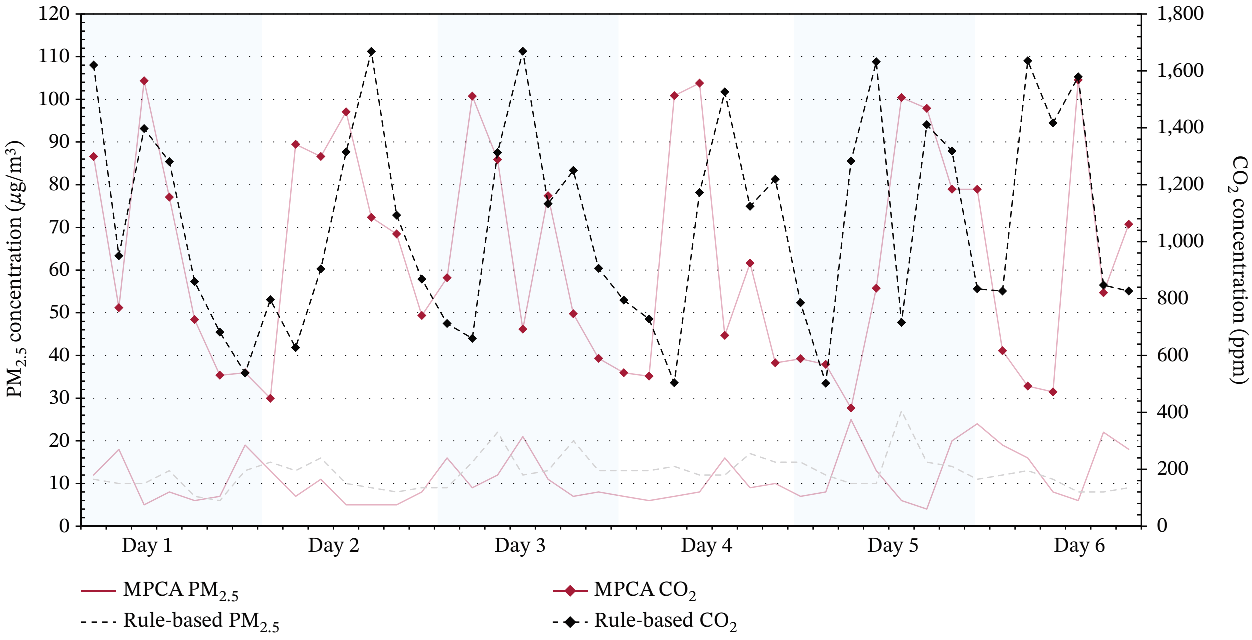

FIGURE 11 | Comparison of the overall $PM_{2.5}$ and CO_2 concentrations according to the control method.

the rule-based control. This is regardless of the primary occupant activity whether it be class hours or nonclass hours. This difference in $PM_{2.5}$ and CO_2 concentrations was greater during class hours than during nonclass hours, suggesting that the MPCA was better suited to supporting IAQ during essential activities during class time for students. Although both MPCA and rule-based control showed significantly higher concentrations of $PM_{2.5}$ and CO_2 than ODC, this is believed to be due to the excessive use of the ventilation system that occurred in ODC classroom as stated earlier.

In all three classrooms, the $PM_{2.5}$ concentrations were lower and CO_2 concentrations were higher during class hours than during nonclass hours. This was due to occupant activity patterns; during class hours, students remained seated and focused on learning, reducing activity levels but increasing respiration. With reduced movement and closed doors and windows, $PM_{2.5}$ entry and resuspension decreased, allowing particles to settle, which lowered the $PM_{2.5}$ concentration. However, the increased respiration and closed environment led to a rise in the CO_2 concentration. In contrast, during nonclass hours, activities such as entering and exiting the classroom caused doors to open, allowing more $PM_{2.5}$ to enter and previously settled particles to be resuspended, thus raising $PM_{2.5}$ levels. Additionally, fewer students remained in the room, reducing CO_2 production from respiration, whereas the open doors and windows allowed the CO_2 to escape, thus reducing the CO_2 concentration.

Additionally, it is worth noticing the improvement of MPCA over rule-based control in sense of duration of maintaining lower levels of $PM_{2.5}$ and CO_2 concentration during class hours. Given that class hours are the most important activity time for students, the MPCA was thus better suited for school facilities than the rule-based algorithm because it maintained an acceptable IAQ for a longer period during class hours.

4.2.2 | Discussions on Energy Consumption Analysis

The MPCA used 5.7% less energy than rule-based control despite operating for a longer time, which was likely due to differences in energy consumption between the system modes. The outdoor air-intake mode uses two fans (SA and EA), whereas the recirculation mode uses a single fan. Thus, the hourly energy consumption under outdoor air-intake mode was 73.6 W for high, 48.4 W for medium, and 33.4 W for low airflow, whereas recirculation mode consumed 27.9, 17.6, and 12.3 W, respectively, meaning that the outdoor air-intake mode was 2.6–2.7 times more energy-intensive than the indoor air-recirculation mode.

The difference in the operating time under the recirculation and outdoor air intake modes between algorithms was likely due to the preemptive control of the MPCA. The outdoor air-intake mode was activated when indoor CO_2 levels exceeded 1500 ppm; however, the MPCA anticipated CO_2 trends through predictive control, initiating ventilation preemptively even when CO_2 levels were below 1500 ppm. As a result, the time that CO_2 remained above 1500 ppm was reduced, leading to a 30% decrease in outdoor air-intake mode compared with the rule-based algorithm. In contrast, the rule-based algorithm only activated the outdoor air-intake mode once CO_2 levels exceeded 1500 ppm, meaning that outdoor air-intake mode was in operation for longer periods.

This analysis demonstrated that using algorithms to control the IAQ can reduce energy consumption by an average of 58.7% compared with manual control. Additionally, even though the MPCA operated for 4.3% longer than the rule-based algorithm, it consumed 5.7% less energy, which is consistent with a recently conducted review of studies that have utilized model prediction control that reported an average reduction in energy consumption of 1%–8% [70]. The AI-based control algorithm used in the present study also produced a 21% improvement in the $PM_{2.5}$ concentration and a 7% improvement in the CO_2 concentration compared with the rule-based algorithm. Future developments in AI performance can also lead to improvements in the prediction accuracy of the models developed for the proposed MPCA, reduce the difficulty of its application, and reduce its energy consumption further.

According to comparative analysis of the operating time and energy consumption by occupant activity type (Table 11 and Figure 6), the order of most common operation mode for MPCA changes between class hours and nonclass hours. This was due to the predictive and preemptive nature of the MPCA, which anticipated higher $PM_{2.5}$ concentrations based on trends from prior nonclass periods and focused on $PM_{2.5}$ reduction during class hours. Toward the end of the class hours, the algorithm shifted focus to CO_2 reduction, which had typically risen by that point. As a result, the ranking of the control modes according to the energy consumption during class hours differed from the ranking for operating time.

On the other hand, the rule-based algorithm shows simpler and synchronized results for the ranking of both operating hours and energy consumption. This is due to the rule-based algorithm operating based on the current concentrations of the IAQ contaminants. During class hours, the focus was primarily on reducing elevated CO_2 levels, leading to the higher use of the outdoor air intake mode. Conversely, during nonclass hours, priority shifted to reducing the $PM_{2.5}$ concentration, resulting in the greater use of recirculation mode.

Analysis on energy consumption during periods when the IAQ met the established threshold according to control algorithm (Figure 7) shows that the MPCA consumes more energy than rule-based algorithm in all three cases. This difference was likely due to the preemptive control of the MPCA, which activated the ventilation system even when the $PM_{2.5}$ concentration was below 15 $\mu g/m^3$ or the CO_2 concentration was below 1500 ppm or both, resulting in higher energy use compared with the rule-based algorithm. To confirm this, a comparison was made of the operation time when the actual $PM_{2.5}$ and CO_2 levels were below the desired set points. Under the MPCA, the system operated for an additional 40 min when the $PM_{2.5}$ concentration was below 15 $\mu g/m^3$, consuming 11.6 W of energy, and for 7 min when the CO_2 levels were below 1500 ppm, consuming 5.6 W.

The comparative analysis on average air quality using control algorithms during periods when the $PM_{2.5}$ and CO_2 concentrations were below the threshold (Table 12 and Figure 8) is subject to discussion. The analysis revealed that MPCA consumed more energy than the rule-based algorithm when the IAQ was within an acceptable range. This is because the MPCA initiated preemptive control, allowing it to activate even when $PM_{2.5}$ or CO_2 or both were within set levels based on values predicted 5 min ahead of time. In addition, the MPCA demonstrated stronger pollutant reduction capabilities than the rule-based algorithm, resulting in a longer period of acceptable IAQ. Although the energy consumption during acceptable IAQ periods was higher for the MPCA, its total energy consumption was still lower than that of the rule-based algorithm.

Additional comparative analysis between the MPCA and rule-based algorithm in terms of temperature has been undertaken, which also shows that MPCA produced a lower average indoor temperature of 25.8°C compared with that of the rule-based algorithm (27.1°C). The MPCA also led to a lower average indoor temperature for class hours (25.9°C) compared with that of the rule-based algorithm (27.3°C). This is because the MPCA had longer operating hours, with its preemptive control leading to the longer use of outdoor air intake mode and the ERV system in general. This indicates that the MPCA can potentially be employed with HVAC systems to reduce thermal energy consumption.

4.2.3 | Discussions on Empirical Experiment Methodology

This empirical experiment was conducted in a single elementary school located in a Dwa climate zone during autumn. In the Korean context, autumn conditions are broadly comparable to that of spring, both representing mild transitional seasons, excluding episodic yellow dust events. Additionally, the autumn conditions are suitable for empirical experiments using elementary school in Korea as it covers majority of school days in second semester while showing less undesirable events schedule wise compared with spring season. Winter and summer periods largely overlap with school vacations, making occupancy-driven IAQ dynamics difficult to capture. Therefore, the findings here should be interpreted as proof-of-concept under midseason conditions. Future research could extend validation to extreme heating (winter) and cooling/high-humidity (summer) periods to confirm generalizability, be as fewer school days as it may in comparison with autumn season, especially to expand research fields into thermal control.

This study addresses several limitations identified in previous IAQ control research and provides a differentiated contribution by implementing and validating an AI-based MPCA in an actual elementary school classroom. For example, this study implements empirical research methodology by utilizing a living-lab elementary school classroom, unlike other research like Choi and Lee [29], or Park et al. [30]. which used computer simulations. Additionally, in comparison with Kim et al. [57], this study focused on controlling both particulate contaminant ($PM_{2.5}$) and gas contaminant (CO_2) instead of focusing on only one. Moreover, this study's empirical experiment can serve as a practical experimentation to existing attempts to consider both IAQ and energy efficiency in school environments like Cho et al. [32]. Therefore, in comparison with previous related research, it can be discussed that this study's several distinctive contributions can be positioned within existing literatures.

5 | Conclusions

In this study, an AI-based prediction control algorithm for an ERV system was developed to manage the indoor environment in elementary school classrooms, with its real-time performance evaluated in the field. Utilizing living-lab classrooms within an actual elementary school, real-time air quality data were collected, and the resulting dataset was employed to develop ANN prediction models for the indoor $PM_{2.5}$ and CO_2 concentrations and temperature. Subsequently, the rule-based MPCA and ODC were compared in three classrooms. The main findings of this study are summarized below.

1. Retraining of the prediction models improved their prediction performance. As a result of this retraining, the CVRMSE for the $PM_{2.5}$ prediction model improved by 22% and its R^2 improved by 14%. Similarly, the CO_2 prediction model demonstrated improvements of 71% and 1%, whereas the temperature prediction model improved by 22% and 34%, respectively. These retrained prediction models were integrated into the MPCA.

2. The living-lab empirical experiment demonstrated that the MPCA combined with the ANN-based prediction models successfully maintained acceptable IAQ levels within the classroom. During the experimental period, the MPCA led to a reduction in the $PM_{2.5}$ and CO_2 concentrations of approximately 21% and 7%, respectively, compared with the rule-based algorithm. Additionally, the MPCA maintained lower indoor $PM_{2.5}$ and CO_2 concentrations for longer periods during class time (45% and 29% longer, respectively) compared with the rule-based algorithm. These findings confirmed that the MPCA was more suitable for school facilities than the rule-based algorithm.

3. This study confirmed that automating the ERV system using the proposed MPCA reduced the energy consumption compared with ODC. The classroom with ODC had energy consumption levels that were 2.4–2.5 times higher than those of the other classrooms because the ERV system operated continuously. In the comparison between algorithms, the MPCA demonstrated a 4.3% longer operating time than the rule-based algorithm, yet had a 5.7% lower energy consumption. This demonstrated that the preemptive control of the MPCA led to a more efficient improvement in the IAQ compared with the traditional rule-based algorithm.

4. The energy consumption of the MPCA was higher than that of the rule-based algorithm when IAQ levels were within the desired range. This is because the MPCA initiated preemptive operation based on predicted values even when the IAQ was satisfactory. However, the overall energy efficiency of the MPCA was higher than that of the rule-based algorithm while also producing a higher IAQ performance.

In summary, the MPCA developed in this study demonstrated superior IAQ performance and lower energy consumption compared with the conventional rule-based algorithm. Using the MPCA for IAQ control was also significantly more efficient in terms of energy consumption compared with ODC while satisfactorily enhancing the IAQ. Therefore, the MPCA developed in this study achieved preemptive IAQ prediction-based control and exhibited a high energy efficiency, positioning it as a promising strategy for improving the IAQ in elementary school facilities.

However, the prediction models used in the MPCA required continuous retraining to enhance their prediction accuracy. In addition, although the developed MPCA included temperature prediction and control strategies based on these predictions, the inability to directly control the HVAC system due to constraints associated with the experimental environment was a clear limitation. Therefore, future research will focus on ongoing data collection and the retraining of the prediction models to improve their accuracy. Additionally, an integrated MPCA for HVAC systems that includes the direct control of the heating and cooling systems is planned for future work.

Author Contributions

Tae Won Kim and Jin Woo Moon designed the study. Jae Yoon Byun and Tae Won Kim developed the methodology and devised the relevant experiments. Jae Yoon Byun collected the required data and performed the analysis. Ji Young Yun and Geun Young Yun contributed to managing and organizing the collected data and visualization. Tae Won Kim and Jin Woo Moon contributed to the theoretical framing of the paper and the interpretation of the data. Jae Yoon Byun produced the manuscript text, and Tae Won Kim, Ji Young Yun, and Jin Woo Moon performed later revisions.

Funding

This study was supported by the National Research Foundation of Korea (NRF) grant funded by the Korean government (MSIT) (RS-2023-00217322).

Conflicts of Interest

The authors declare no conflicts of interest.

Data Availability Statement

The data that support the findings of this study are available from the corresponding author upon reasonable request.

References

1. C. Schweizer, R. D. Edwards, L. Bayer-Oglesby, et al., "Indoor Time–Microenvironment–Activity Patterns in Seven Regions of Europe," *Journal of Exposure Science & Environmental Epidemiology* 17, no. 2 (2007): 170–181, https://doi.org/10.1038/sj.jes.7500490.

2. N. E. Klepeis, W. C. Nelson, W. R. Ott, et al., "The National Human Activity Pattern Survey (NHAPS): A Resource for Assessing Exposure to Environmental Pollutants," *Journal of Exposure Science & Environmental Epidemiology* 11, no. 3 (2001): 231–252, https://doi.org/10.1038/sj.jea.7500165.

3. Daegu Catholic University, *Personal Exposure Evaluation Report Based on Citizens' Daily Time-Activity Pattern* (National Institute of Environmental Research, 2010).

4. S. Y. Kim, W. H. Jheong, M. H. Kwon, et al., *A Study on the Microbial Management of Living Space Air Quality* (National Institute of Environmental Research, 2014).

5. S. H. Park, T. H. Park, S. J. Park, et al., "Levels of the Concentration of PM_{10} and $PM_{2.5}$ in Elementary School Classroom at Yeongwol County," *Journal of Odor and Indoor Environment* 17, no. 1 (2018): 11–17, https://doi.org/10.15250/joie.2018.17.1.11.

6. United States Environmental Protection Agency, *Protecting Children's Health During and After Natural Disaster: Extreme Heat Article on Children's Health* (United States Environmental Protection Agency, 2024), https://www.epa.gov/children/protecting-childrens-health-during-and-after-natural-disasters-extreme-heat.

7. W. H. Yang, J. R. Sohn, J. H. Kim, B. S. Son, and J. C. Park, "Indoor Air Quality Investigation According to Age of the School Buildings in Korea," *Journal of Environmental Management* 90, no. 1 (2009): 348–354, https://doi.org/10.1016/j.jenvman.2007.10.003.

8. J. W. Jeong, and H. K. Lee, "Study on the Characteristics of Air Quality in the Classroom of Elementary School and Its Control Methods," *Journal of Korean Society of Environmental Engineering*

32, no. 4 (2010): 311–322, https://www.dbpia.co.kr/journal/articleDetail?nodeId=NODE06752497.

9. Ministry of Environment of Korea, *High Concentration PM Response Manual for Protection of Health Vulnerable Class Such as Children·Student·Elderly* (Ministry of Environment of Korea, 2016).

10. Kweather, YTN Science, *Decrease in Children's Educational Achievements, the Result Lies in Indoor Air Quality?* (Kweather, YTN Science, 2016).

11. W. H. Yang, "School Indoor Air Quality and Health Effects," *Journal of Environmental Health Sciences* 35, no. 3 (2009): 143–152, https://doi.org/10.5668/JEHS.2009.35.3.143.

12. L. Morawska, J. Allen, W. Bahnfleth, et al., "Mandating Indoor Air Quality For Public Buildings," *Science* 383, no. 6690 (2024): 1418–1420, https://doi.org/10.1126/science.adl0677.

13. World Health Organization, *Air Quality Guideline for Europe* (World Health Organization, 1987).

14. Environmental Protection Ageny, *IAQ Standards and Guidelines* (Environmental Protection Ageny, 2006).

15. ASHARE, *Standard 62.1 & 62.2* (ASHARE, 1973).

16. Ministry of Health and Welfare, *Law for Maintenance of Sanitation in Buildings* (Ministry of Health and Welfare, 1970).

17. Ministry of Environment, *Indoor Air Quality Management Act* (2011): Ministry of Environment.

18. H. Grunenberg, and U. Kuckartz, *Umweltbewusstsein Im Wandel: Ergebnisse Der UBA-Studie Umweltbewusstsein In Deutschland 2002* (Springer, 2003), https://doi.org/10.1007/978-3-322-97605-5.

19. O. Seppanen, R. Ruotsalainen, and L. Sarajarvi, *Classification Of Indoor Climate, Construction, And Finishing Materials* (Finnish Society of Indoor Air Quality and Climate, 1995).

20. S. Dimitroulopoulou, M. R. Dudzińska, L. Gunnarsen, et al., "Indoor Air Quality Guidelines From Across the World: An Appraisal Considering Energy Saving, Health, Productivity, and Comfort," *Environment International* 178 (2023): 108127, https://doi.org/10.1016/j.envint.2023.108127.

21. Ministry of Environment, *Indoor Air Quality Management Act* (Ministry of Environment, 2022).

22. Ministry of Education, *School Facility High-Concentration PM Counteract Measures* (Ministry of Education, 2018).

23. W. H. Yang, "Time-Activity Pattern of Students and Indoor Air Quality of School," *Journal of Korean Institute of Educational Facilities* 21, no. 6 (2014): 17–22.

24. "Korea Heating, Air-Conditioning, Refrigeration & Renewable Energy News. (2019). School Air Quality Solution 'Ventilation'...What's the Market Response Plan?," https://kharn.kr/mobile/article.html?no=8670.

25. Y. An, Z. Niu, and C. Chen, "Smart Control of Window and Air Cleaner for Mitigating Indoor PM2.5 With Reduced Energy Consumption Based on Deep Reinforcement Learning," *Building and Environment* 224 (2022): 109583, https://doi.org/10.1016/j.buildenv.2022.109583.

26. Y. J. Choi, E. J. Choi, H. W. Cho, and J. W. Moon, "Development of an Indoor Particulate Matter (PM2.5) Prediction Model for Improving School Indoor Air Quality Environment," *KIEAE Journal* 21, no. 1 (2021): 35–40, https://doi.org/10.12813/kieae.2021.21.1.035.

27. M. K. Kim, and C. E. Hong, "The Artificial Neural Network Based Electric Power Demand Forecast Using a Season and Weather Informations," *Journal of the Institute of Electronics and Information Engineers* 53, no. 1 (2016): 71–78, https://doi.org/10.5573/ieie.2016.53.1.071.

28. B. Lagesse, S. Wang, T. V. Larson, and A. A. Kim, "Predicting PM2.5in Well-Mixed Indoor Air for a Large Office Building Using Regression and Artificial Neural Network Models," *Environmental Science & Technology* 54, no. 23 (2020): 15320–15328, https://doi.org/10.1021/acs.est.0c02549.

29. Y. Y. Choi, and H. S. Lee, "Intelligent and Responsive Window Opening-Closing Operation Process for Carbon Dioxide (CO2) Management of Secondary School Classroom," *Journal of the Korean Institute of Educational Facilities* 25, no. 4 (2018): 19–30, https://doi.org/10.7859/kief.2018.25.4.019.

30. H. C. Park, D. H. Lee, and J. J. Yee, "A Study on Development and Application of Sequential Control Algorithm of Ventilation and Air Cleaning System for Improving Indoor Air Quality in School Classroom," *Journal of the Architectural Institute of Korea Structure & Construction* 36, no. 5 (2020): 187–194, https://doi.org/10.5659/JAIK_SC.2020.36.5.187.

31. F. Stazi, F. Naspi, G. Ulpiani, and C. Di Perna, "Indoor Air Quality and Thermal Comfort Optimization in Classrooms Developing an Automatic System for Windows Opening and Closing," *Energy and Building* 139 (2017): 732–746, https://doi.org/10.1016/j.enbuild.2017.01.017.

32. J. Cho, Y. Heo, and J. W. Moon, "An Intelligent HVAC Control Strategy for Supplying Comfortable and Energy-Efficient School Environment," *Advanced Engineering Informatics* 55 (2023): 101895, https://doi.org/10.1016/j.aei.2023.101895.

33. N. Clements, R. Zhang, A. Jamrozik, C. Campanella, and B. Bauer, "The Spatial and Temporal Variability of the Indoor Environmental Quality During Three Simulated Office Studies at a Living-Lab," *Buildings* 9, no. 3 (2019): 62, https://doi.org/10.3390/buildings9030062.

34. M. Zinzi, M. Botticelli, F. Fasano, P. Grasso, and G. Chiesa, "Comparing the Thermal Performance of Living-Lab Monitoring and Simulation With Different Level of Input Detail," *E3S Web of Conferences* 396 (2023): 04002, https://doi.org/10.1051/e3sconf/202339604002.

35. S. H. Hong, E. H. Jang, J. H. Cho, et al., "A Living-Lab to Develop Smart Home Services for the Residential Welfare of Older Adults," *Technology in Society* 77 (2024): 102577, https://doi.org/10.1016/j.techsoc.2024.102577.

36. J. Y. Kim, S. A. Kim, S. J. Bae, M. J. Kim, Y. B. Cho, and K. I. Lee, "Indoor Environment Monitoring System Tested in a Living-Lab," *Building and Environment* 214 (2022): 108879, https://doi.org/10.1016/j.buildenv.2022.108879.

37. F. L. Plazas, and C. S. de Tejada, "Natural Ventilation to Improve Indoor Air Quality (IAQ) in Existing Homes: The Development of Health-Based and Context-Specific User Guidelines," *Energy and Buildings* 314 (2024): 114248, https://doi.org/10.1016/j.enbuild.2024.114248.

38. W. Shang, J. Liu, C. Wang, J. Li, and X. Dai, "Developing Smart Air Purifier Control Strategies for Better IAQ and Energy Efficiency Using Reinforcement Learning," *Building and Environment* 242 (2023): 110556, https://doi.org/10.1016/j.buildenv.2023.110556.

39. L. A. El-Leathey, P. Anghelita, A. L. Constantin, G. Circiumaru, and R. A. Chihaia, "System for Indoor Comfort and Health Monitoring Tested in Office Building Environment," *Applied Sciences* 13, no. 20 (2023): 11360, https://doi.org/10.3390/app132011360.

40. T. W. Kim, and J. H. Lee, "Comparison of Indoor $PM_{2.5}$ Prediction Performance During Occupancy Time Based on Artificial Neural Network Models," *Land and Housing Review* 16, no. 1 (2025): 127–139, https://doi.org/10.5804/LHR.2025.16.1.127.

41. H. Na, H. Choi, H. Kim, D. Park, J. Lee, and T. Kim, "Optimizing Indoor Air Quality and Noise Levels in Old School Classrooms With Air Purifiers and HRV: A CONTAM Simulation Study," *Journal of Building Engineering* 73 (2023): 106645, https://doi.org/10.1016/j.jobe.2023.106645.

42. L. Jia, J. Han, X. Chen, Q. Li, C. Lee, and Y. Fung, "Interaction Between Thermal Comfort, Indoor Air Quality and Ventilation Energy Consumption of Educational Buildings: A Comprehensive

Review," *Buildings* 11, no. 12 (2021): 591, https://doi.org/10.3390/buildings11120591.

43. S. Sadrizadeh, R. Yao, F. Yuan, et al., "Indoor Air Quality and Health in Schools: A Critical Review for Developing the Roadmap for the Future School Environment," *Journal of Building Engineering* 57 (2022): 104908, https://doi.org/10.1016/j.jobe.2022.104908.

44. T. Al Mindeel, E. Spentzou, and M. Eftekhari, "Energy, Thermal Comfort, and Indoor Air Quality: Multi-Objective Optimization Review," *Renewable and Sustainable Energy Reviews* 202 (2024): 114682, https://doi.org/10.1016/j.rser.2024.114682.

45. K. Yu, Y. Chen, E. Jaimes, et al., "Optimization of Thermal Comfort, Indoor Quality, and Energy-Saving in Campus Classroom Through Deep Q Learning," *Case Studies in Thermal Engineering* 24 (2021): 100842, https://doi.org/10.1016/j.csite.2021.100842.

46. D. W. Park, S. H. Kim, and H. J. Yoon, "The Impact of Indoor Air Pollution on Asthma," *Allergy Asthma Respiratory Disease* 5, no. 6 (2017): 312, https://doi.org/10.4168/aard.2017.5.6.312.

47. S. M. Almeida, T. Faria, V. Martins, et al., "Source Apportionment of Children Daily Exposure to Particulate Matter," *Science of The Total Environment* 835 (2022): 155349, https://doi.org/10.1016/j.scitotenv.2022.155349.

48. J. Lee, T. Wan Kim, C. Lee, and C. Koo, "Integrated Approach To Evaluating The Effect Of Indoor CO2 Concentration On Human Cognitive Performance And Neural Responses In Office Environment," *Journal of Management in Engineering* 38, no. 1 (2022): 04021085, https://doi.org/10.1061/(ASCE)ME.1943-5479.0000993.

49. Y. S. Son, "Particulate Matter and Influencing Factors in Domestic Elementary Schools," *Journal of Korean Society for Atmospheric Environment* 36, no. 2 (2020): 153–170, https://doi.org/10.5572/KOSAE.2020.36.2.153.

50. D. S. Kim, Y. A. Choi, and T. J. Lee, "Investigation of Indoor Air Quality and Characteristics of PMs Concentration Followed by Indoor Activities in Preschool," *Journal of Korean Society for Indoor Environment* 3, no. 3 (2006): 273–284https://db.koreascholar.com/Article/Detail/31643.

51. A. P. Jones, "Indoor Air Quality and Health," *Atmospheric Environment* 33, no. 28 (1999): 4535–4564, https://doi.org/10.1016/S1352-2310(99)00272-1.

52. M. Maroni, B. Seifet, and T. Linvall, *Indoor Air Quality, a Comprehensive Reference Book Air Quality Monographs* (Institute International of Refrigeration, 1995).

53. S. Kim, K. Kang, D. Park, and T. Kim, "Assessment Of PM2. 5 Penetration Based On Airflow Paths In Korean Classrooms," *Building and Environment* 248 (2024): , https://doi.org/10.1016/j.buildenv.2023.111103111103.

54. S. Heo, D. Y. Kim, Y. Kwoun, T. J. Lee, and Y. M. Jo, "Characterization of Classroom Fine Dust in Urban Elementary Schools," *Atmospheric Environment* 37, no. 1 (2021): 113–124, https://doi.org/10.5572/KOSAE.2021.37.1.113.

55. H. S. Song, "Comparison of Performance Between MLP and RNN Model to Predict Purchase Timing for Repurchase Product," *Journal of Information Technology Applications and Management* 24, no. 1 (2017): 111–128, https://doi.org/10.21219/JITAM.2017.24.1.111.

56. J. Dong, N. Goodman, and P. Rajagopalan, "A Review of Artificial Neural Network Models Applied to Predict Indoor Air Quality in Schools," *International Journal of Environmental Research and Public Health* 20, no. 15 (2023): 6441, https://doi.org/10.3390/ijerph20156441.

57. T. W. Kim, J. Y. Byun, J. Y. Yun, Y. G. Jung, and J. W. Moon, "Performance Analysis of Particulate Matter Priority Control Algorithm for Outdoor Air-Introduced Ventilation Cleaner Using Prediction Model," *Energy and Buildings* 324 (2024): 114885, https://doi.org/10.1016/j.enbuild.2024.114885.

58. J. H. Kim, *Ventilation and Filtration Control Strategy Considering Indoor and Outdoor Particle Environmental Conditions of Apartment Building* (Seoul University Doctorate Paper, 2018).

59. J. Snoek, H. Larochelle, and R. P. Adams, "Practical Bayesian Optimization of Machine Learning Algorithms," *Advances in Neural Information Processing System* 25 (2012): .

60. D. P. Kingma, and J. L. Ba, "Adam: A Method for Stochastic Optimization," (2014) 1412 (2014): https://arxiv.org/abs/1412.6980.

61. A. R. Ismail, M. Z. R. Azhary, and N. A. Hitam, "Evaluating Adan vs. Adam: An Analysis of Optimizer Performance in Deep Learning," in *International Symposium on Intelligent Computing Systems* (Cham: Springer Nature Switzerland, 2024).

62. M. Stafoggia, J. Schwartz, C. Badaloni, et al., "Estimation of Daily PM10 Concentrations in Italy (2006-2012) Using Finely Resolved Satellite Data Land Use Variables and Meteorology," *Environment International* 99 (2017): 234–244.

63. K. P. Murphy, *Machine Learning: A Probabilistic Perspective* (MIT press, 2012).

64. Y. M. Wi, K. B. Song, and S. K. Joo, "Load Forecasting for the Holidays Using a Data Mining With the Coefficient of Determination," *Institute of Electrical Engineers* (2008): 552–553, https://www.dbpia.co.kr/journal/articleDetail?nodeId=NODE01299462.

65. S. D. Lowther, S. Dimitroulopoulou, K. Foxall, et al., "Low-Level Carbon Dioxide Indoors: A Pollution Indicator or a Pollutant? A Health-Based Perspective," *Environments* 8, no. 11 (2021): 125, https://doi.org/10.3390/environments8110125.

66. C. Liedtke, M. Jolanta Welfens, H. Rohn, and J. Nordmann, "LIVING LAB: User-Driven Innovation for Sustainability," *International Journal of Sustainability in Higher Education* 13, no. 2 (2012): 106–118, https://doi.org/10.1108/14676371211211809.

67. J. M. Park, S. H. Park, S. W. Park, and D. S. Song, "Simulation Analysis of Indoor PM Reduction Effect by Installing an Air Curtain in a Daycare Center, Korean," *Journal of Air-Conditioning and Refrigeration Engineering* 33 (2021): .

68. D. Mei, X. Zhang, C. Wang, L. Liu, and J. Li, "Multi-Objective Ventilation Optimization for Indoor Air Quality, Thermal Comfort, and Energy Conservation in the Post-Pandemic Era: A Case Study for a Moving Elevator," *Physics of Fluids* 36, no. 6 (2024): .

69. K. Aydin, and B. Yilmaz, "CFD-Based Multi-Objective Optimization of Indoor Air Quality and Thermal Comfort in a Classroom," *Proceedings of the Institution of Mechanical Engineers, Part E: Journal of Process Mechanical Engineering* 238, no. 5 (2024): 2511–2523.

70. J. Saini, M. Dutta, and G. Marques, "Indoor Air Quality Prediction Systems for Smart Environments: A Systematic Review," *Journal of Ambient Intelligence and Smart Environments* 12, no. 5 (2020): 433–453, https://doi.org/10.3233/AIS-200574.